NASA

Technical Memorandum 83922

Numerical Prediction of the Mid-Atlantic States Cyclone of 18-19 February 1979

Robert Atlas and Robert Rosenberg

January 1982

Laboratory for Atmospheric Sciences
Modeling and Simulation Facility

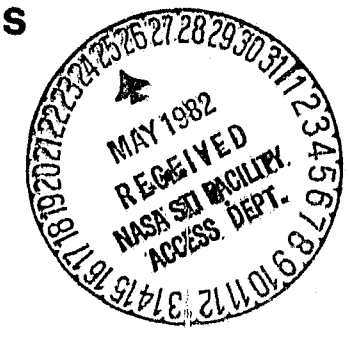

National Aeronautics and
Space Administration

Goddard Space Flight Center
Greenbelt, Maryland 20771

Numerical Prediction of the Mid-Atlantic States Cyclone of 18-19 February 1979

Robert Atlas

Goddard Laboratory for Atmospheric Sciences
NASA/Goddard Space Flight Center
Greenbelt, Maryland 20771

and

Robert Rosenberg

Sigma Data Services Corporation
NASA/Goddard Space Flight Center
Greenbelt, Maryland 20771

January 1982

ABSTRACT

A series of forecast experiments was conducted to assess the accuracy of the GLAS model's prediction of the Mid-Atlantic States cyclone of 18-19 February 1979, and to determine the importance of large-scale dynamical processes and diabatic heating to the cyclogenesis. The GLAS model forecast from the GLAS analysis at 0000 GMT 18 February correctly predicted intense coastal cyclogenesis and heavy precipitation. When this forecast was repeated without surface heat and moisture fluxes, the model failed to predict any cyclone development. An extended-range forecast from 0000 GMT 16 February as well as a forecast from the NMC analysis at 0000 GMT 18 February interpolated to the GLAS grid and a forecast from the GLAS analysis at 0000 GMT 18 February with the surface moisture flux excluded predicted weak coastal low development.

Examination of these forecasts shows that diabatic heating resulting from oceanic fluxes significantly contributed to the generation of low level cyclonic vorticity and the intensification and slow rate of movement of an upper level ridge over the western Atlantic. As an upper level short-wave trough approached this ridge, diabatic heating associated with the release of latent heat intensified, and the gradient of vorticity, vorticity advection and upper level divergence in advance of the trough were greatly increased, providing strong large-scale forcing for the surface cyclogenesis.

CONTENTS

1. INTRODUCTION

In recent years numerical weather prediction (NWP) models have demonstrated considerable success in the prediction of extratropical cyclone development and displacement. However, notable exceptions occasionally occur in which there are large errors in the predicted location or intensity of cyclogenesis, or the displacement of existing or newly developed cyclones. These errors may be due to a variety of reasons; the most important of which are poor specification of the initial state, numerical errors and inaccurate physical parameterizations. In addition, when cyclogenesis occurs over oceanic regions, the description of the sequence of processes leading to the observed development may be difficult and the exact mechanism of cyclogenesis poorly understood.

A considerable discussion and controversy has developed regarding the development of the Mid-Atlantic States cyclone of 18–19 February 1979. This storm, also referred to as the Presidents' Day cyclone, is significant because of the severity of the weather it produced and the failure of the operational models in use at the National Meteorological Center (NMC) to adequately predict the intensity of cyclogenesis. Excellent reviews of the synoptic situation and development of this storm, have been provided by Bosart (1981) and Uccellini et al. (1981). Both articles also suggested hypotheses for the poor numerical prediction, based on subsynoptic scale phenomena not well represented by the operational models. Bosart emphasized the development of a coastal front and the importance of boundary layer processes to the cyclogenesis, while Uccellini et al. stressed the complex interactions associated with a propagating jet streak. NMC has also conducted experiments relating to this case (J. Newell, personal communication). These experiments show improved short-range (24 h) predictions with a model having higher vertical resolution than the one applied operationally at NMC.

The objective of this paper is to explore the development of this cyclone as predicted by the GLAS general circulation model. Forecasts from 0000 GMT 16 February and 18 February 1979 were performed using different initial analyses and physical parameterizations. Based on these forecasts, the systems and processes which appear to be important to the intensity of cyclogenesis in this case will be discussed.

Sections 2 and 3 present a brief review of the synoptic situation and NMC model forecasts for this case. Descriptive results from the GLAS model forecasts are presented in section 4. Conclusions follow in section 5.

2. SYNOPTIC SITUATION

Detailed descriptions of the synoptic situation for this case have been presented by Bosart and Uccellini et al. Therefore only a brief summary of the main synoptic features will be given here.

Figs. 1 to 5 present the National Weather Service's surface, 850 mb and 500 mb analyses at 12 h intervals for the period 0000 GMT 18 February to 0000 GMT 20 February 1979. At 0000 GMT 18 February (Fig. 1), a massive high pressure system was centered over the Great Lakes. Associated with this system were extremely cold temperatures over the northeast United States and an unusually strong flow of cold dry air over the warm waters adjacent to the east coast. A cold front extended westward from the southern edge of this cold air outbreak to the Gulf of Mexico, while a weak inverted trough extended northward from this front to Kentucky. Weak wave formation was occurring in the Gulf of Mexico in conjunction with moderate cold advection in that area.

At 850 mb, a strong baroclinic zone extended northward from the surface cold front. Nearly zonal flow was present at 500 mb above this zone and a distinct short-wave trough was located over the Great Plains. Light to moderate

snow was occurring beneath and slightly in advance of this upper level trough while primarily drizzle and rain was falling in the vicinity of the surface inverted trough.

During the next 12 h (Fig. 2), the surface high moved slowly eastward, the inverted trough extending northward from the Gulf of Mexico intensified, a weak low appeared along the frontal wave in the Gulf, and a coastal front (not evident in the synoptic scale analysis of available conventional data) developed along the southeast coast. The strong cold advection which had been prevalent at 850 mb along nearly the entire east coast ended in that area due to the eastward movement of the high. This was replaced by strong warm advection along the South Carolina coast where 50 knot winds from the southeast were reported at the 850 mb level. At 500 mb, the short-wave trough deepened and moved slowly eastward. A shallow ridge, downstream from this trough moved over the eastern United States accompanied by west-northwesterly flow over the east coast and adjacent waters. Precipitation, primarily in the form of snow at 1200 GMT 18 February covered most of the southeast and extended northwestward to the Great Plains.

By 0000 GMT 19 February (Fig. 3), a new surface low with a central pressure of approximately 1017 mb formed along the coastal front, while a much weaker pressure minimum appeared over Kentucky within the inverted trough to its northwest. These systems were separated by a shallow wedge of cold air which had moved southward along the lee side of the Appalachian mountains during the preceding 12 h. At 850 mb, a low pressure center was located along the Illinois-Indiana border just slightly to the west of the weak surface low in Kentucky, while warm advection was occurring above and slightly to the north of the coastal low. At 500 mb, the short-wave trough had continued to move eastward and was located directly above the 850 mb low, and nearly

straight west-southwesterly flow was present above the coastal low. At this time, moderate to heavy snow was occurring in portions of Virginia and North Carolina, while light to moderate snow extended to the northwest of this area.

During the next 9 h, the low previously over Kentucky moved northeastward to Ohio without substantially changing in intensity, while the coastal low moved northward to Cape Hatteras and deepened slightly. Following 0900 GMT 19 February, explosive cyclone development began to the north of Cape Hatteras in conjunction with the movement of the upper level short-wave trough toward this area and the shortening of the half-wavelength between this trough and the offshore ridge. At 1200 GMT 19 February (Fig. 4), an intense surface low with a central pressure of approximately 1006 mb was located due east of Virginia under the diffluent flow in advance of the 500 mb trough. A strong cyclonic circulation was also present at 850 mb, with the low pressure center at this level located slightly to the west of the surface low. A baroclinic thermal structure is evident with the low located between an upstream thermal trough and downstream thermal ridge. Heavy snow was occurring from Virginia to southeast New York at this time.

The surface low moved slowly to the east-northeast and continued to deepen rapidly for the next 6 h but underwent little change in intensity thereafter. By 0000 GMT 20 February (Fig. 5), the intense cyclone and the 500 mb short-wave trough had moved well offshore and snow had ended along the entire east coast.

3. NMC MODEL FORECASTS

In recent years, NMC's primitive equation models have shown outstanding success in the prediction of intense winter storms (Cressman, 1978). In addition, while the Barotropic model is not capable of directly forecasting cyclogenesis, it can and often does provide strong indications that cyclone development will

occur. This is usually apparent as the shortening of the half-wavelength between a trough and downstream ridge or by the amplification of a trough with attendant increased positive vorticity advection over a surface baroclinic zone (Staff, National Weather Analysis Center, 1960).

The Barotropic model, Limited-area Fine Mesh model (LFM-II), and Seven-Level Primitive Equation models in use at the National Meteorological Center in February 1979, all failed to provide accurate prognostic guidance for the intensity of cyclone development that occurred on 19 February.

Fig. 6 shows the Barotropic model's initial analysis of 500 mb geopotential height and absolute vorticity on 0000 GMT 18 February, its 36 h forecast from this initial condition, and the verifying barotropic analysis for 1200 GMT 19 February. Comparison of these figures reveals that the Barotropic model did not predict the intensification of the short-wave trough or the development of an offshore ridge. As a result it greatly underestimated the gradient of vorticity and the vorticity advection in the region of cyclone development.

Figs. 7 and 8 show the LFM-II's 12 h, 24 h, and 36 h forecasts of sea-level pressure and 500 geopotential height and absolute vorticity valid at 1200 GMT 19 February as well as the verifying analyses for that time. Comparison of the sea-level pressure predictions (Fig. 7) with the verification shows a considerable improvement in forecast accuracy with time but reveals serious deficiencies in all of the forecasts. The 12 h forecast correctly predicted that cyclogenesis would occur but significantly underestimated the intensity of cyclone development and incorrectly indicated the position of the low too far south. The 24 h forecast also predicted cyclone development but indicated an even weaker cyclonic circulation; the 36 h forecast predicted only an inverted trough along the east coast.

Part of the explanation for the errors at sea level is evident from the LFM-II's 500 mb height and vorticity prognoses (Fig. 8). Comparison of these forecasts with the verification shows that although the prediction of the amplitude of the short-wave trough and associated vorticity maximum improves with time and is significantly better than the Barotropic model's prediction, all of the forecasts substantially underestimate the development of the offshore ridge. As a result, the gradient of vorticity, vorticity advection and upper level divergence in advance of the trough are also underestimated.

4. GLAS MODEL FORECASTS

The objectives of our experiments were to assess the accuracy of the GLAS model's prediction and determine the importance of large-scale processes and diabatic heating to the development. In this section, GLAS model forecasts from 0000 GMT 16 February and 18 February 1979, will be presented. Initial conditions for the forecasts were provided by either the GLAS NOSAT assimilation cycle (described in detail by Halem et al., 1982) which began on 5 January and continued through 5 March 1979, or by an interpolation of the NMC analysis to the GLAS grid.

In the GLAS objective analysis scheme (Baker et al., 1981), zonal and meridional wind components, geopotential height and relative humidity are analyzed on mandatory pressure surfaces. The 6 h model forecast provides a first guess for these fields at 300 mb and at sea level, where pressure and temperature are also analyzed. The first guess for the other levels is obtained from the model first guess, modified by a vertical interpolation between the two closest completed analyses. Vertical consistency is maintained through static stability constraints. The analysis at each level is performed with a successive correction method (Cressman, 1959) modified to account for differences in the data density and the statistical estimates of the error structure of the observations.

The model used in the assimilation and to generate the forecasts is the fourth order global atmospheric model described by Kalnay-Rivas et al. (1977), Kalnay-Rivas and Hoitsma (1979) and Halem et al. (1982). It has nine vertical layers, equally spaced in sigma, and a rather coarse horizontal resolution of 4° latitude by 5° longitude, which is compensated by the use of accurate horizontal differences. With the exception of the computation of longwave radiation (Wu, 1980), and a slight change to the calculation of surface temperature and surface fluxes (Sud and Abeles, 1981), the parameterization of physical processes is essentially the same as in the second order model of Somerville et al.(1974).

Table 1 summarizes the forecast experiments that were performed. Complete model physics was used in all but two of the forecasts. In one of the experiments sensible and latent heat fluxes from the earth's surface to the atmosphere were eliminated; in the other experiment, only the latent heat flux was removed.

a. Forecasts from 0000 GMT 18 February 1979.

Figs. 9 and 10 present the sea-level pressure, 1000-500 mb thickness, 850 mb geopotential height and temperature and 500 mb geopotential height and temperature fields from the GLAS NOSAT analysis and the NMC analysis interpolated to the GLAS grid at 0000 GMT 18 February 1979. Comparison of these figures shows little difference in the representation of the anticyclone over the northeast, the baroclinic zone along the east coast or the inverted trough extending northward from the Gulf of Mexico. However, at 500 mb the GLAS NOSAT analysis portrays a somewhat stronger short-wave trough along 100° W than does the interpolated NMC analysis.

FORECAST FROM THE GLAS ANALYSIS

Figs. 11 to 14 show the 12 h to 48 h forecasts of sea level pressure, 1000-500 mb thickness, 850 mb geopotential height and temperature and 500 mb geopotential height and temperature from the GLAS NOSAT analysis at 0000 GMT 18 February 1979 at 12 h intervals. During the first 12 h of the forecast (Fig. 11), the anticyclone initially over the Great Lakes as well as the inverted trough extending northward from the Gulf of Mexico are predicted to move slowly eastward, and a new inverted trough begins to develop along the southeast coast of the United States. At 850 mb, strong cold advection ends along most of the east coast as a ridge moves over this area. At 500 mb, the short wave trough moves slowly eastward and a ridge moves over the eastern United States.

Over the next 12 h, the offshore inverted trough at the surface intensifies and general eastward propogation of the 500 mb trough and ridge, the surface anticyclone and the inverted trough over the southeast continues. The forecast for 0000 GMT 19 February (Fig. 12) shows the surface anticyclone to be over the northeast and a single broad inverted trough along the east coast. At 850 mb a moderate cyclonic circulation is centered over the Ohio Valley directly beneath the 500 mb short-wave trough. A shallow 500 mb ridge is located along the east coast.

Weak surface cyclogenesis and moderate precipitation (not shown) begins within the inverted trough along the east coast during the next 3 h and dramatically intensifies 3 h to 6 h later with the approach of the upper level trough toward this area. The forecast for 1200 GMT 19 February (Fig. 13) shows an intense surface cyclone with a central contour value of 1012 mb located just offshore from the Virginia-North Carolina coast. The surface low pressure center is located slightly upstream from the 1000-500 mb thickness

ridge in a region of positive thermal vorticity advection. At 850 mb, there is a strong cyclonic circulation centered slightly to the west of the surface low and also upstream from the thermal ridge. At 500 mb, the short-wave trough is located over the Appalachian mountains while the ridge at this level is to the east of the surface cyclone. The half-wavelength between the trough and downstream ridge has been predicted to decrease slightly and diffluent flow from the southwest exists over the intensifying low. Heavy precipitation (not shown) was predicted to occur along the mid-Atlantic coast from Virginia to New York at this time.

During the next 12 h of the forecast (Fig. 14), the 500 mb trough moves to the east coast and the surface cyclone moves to the northeast while continuing to intensify. At 0000 GMT 20 February the surface low is predicted to have a central contour value of 1004 mb and to now be located within the 1000-500 mb thickness ridge. The 850 mb low is also predicted to have a warm core structure at this time.

FORECASTS FROM THE GLAS ANALYSIS WITHOUT SURFACE HEAT AND/OR MOISTURE FLUXES

Figs. 15 to 18 present the 12 h, 24 h, 36 h and 48 h forecasts from the GLAS analysis at 0000 GMT 18 February in which surface sensible and latent heat fluxes were eliminated from the model. The 12 h forecast (Fig. 15) shows the slow eastward movement of the surface anticyclone, the 850 mb ridge and the 500 mb short-wave trough and ridge but does not indicate the development of an inverted trough at the surface along the southeast coast. Instead the surface high becomes well established over the coastal waters.

During the next 24 h (figs. 16 and 17), the inverted trough extending northward from the Gulf of Mexico is forecast to decrease in amplitude and remain quasi-stationary despite the movement of the surface high offshore. At 850 mb a moderately strong cyclonic circulation is forecast to develop

over the midwest and move eastward. At 500, mb the short-wave trough is forecast to move over the eastern United States as the ridge at this level weakens slightly and moves well offshore. The half-wavelength between the trough and downstream ridge is predicted to increase and surface cyclogenesis does not occur. Over the next 12 h, (Fig. 18) the surface high continues to move eastward leaving a weak pressure gradient over the east coast, and the 850 mb and 500 mb troughs weaken and move offshore.

Figs. 19-22 show the 12 h to 48 h forecasts from the GLAS analysis at 0000 GMT 18 February in which only the surface latent heat flux was eliminated from the model. This forecast is similar to the preceding GLAS model predictions at 850 mb and 500 mb during the first 24 h, but differs at the surface in its development of a somewhat weaker inverted trough along the southeast coast than is present in the forecast which included both sensible and latent heat fluxes. From 24 h to 36 h, the surface inverted trough amplifies markedly, but cyclogenesis does not occur as the upper level trough approaches the east coast and the half-wavelength between this trough and the weakening ridge increases slightly. During the last 12 h of the forecast a weak low with a central contour value of 1024 mb is predicted to develop within the inverted trough at the surface.

FORECAST FROM THE NMC ANALYSIS

Figs. 23-25 show the 12 h, 24 h and 36 h forecasts from the interpolated NMC analysis. During the first 24 h of the forecast (Figs. 23 and 24), a broad inverted trough, which is slightly weaker than in the corresponding forecast from the GLAS analysis, forms at the surface over the southeast United States and adjacent waters as an eastward moving inverted trough merges with a developing coastal trough. The short-wave trough at 500 mb is predicted to move to the Ohio Valley and weaken while a shallow ridge at this level moves

over the east coast. As the upper level trough approaches the east coast, cyclogenesis is predicted to occur within the inverted trough, such that by 1200 GMT 19 February (Fig. 25) a surface cyclone with a central contour value of 1020 mb is forecast to the east of the North Carolina coast. A closed low pressure center was not predicted to form at 850 mb, although a moderately strong cyclonic circulation with favorable baroclinic thermal structure is indicated.

b. Forecast from the GLAS analysis at 0000 GMT 16 February 1979.

Figs. 26-29 present the 48 h to 84 h forecasts of sea-level pressure, 1000-500 mb thickness, 850 mb geopotential height and temperature and 500 mb height and temperature from 0000 GMT 16 February 1979 at 12 h intervals. The 48 h forecast (Fig. 26) correctly shows the massive anticyclone which dominated the northeast United States, the strong cold air outbreak along nearly the entire east coast and the inverted trough extending northward from the Gulf of Mexico. However, at 500 mb a very serious error is present as the model has predicted only very shallow troughing over the central plains. Over the next 24 h (Figs. 27 and 28) the surface high moves slowly eastward and a broad inverted trough develops over the east coast under nearly straight west-northwesterly flow aloft. Weak cyclogenesis is predicted to occur within this inverted trough during the next 12 h as the shallow upper-level trough moves toward the east coast. By 1200 GMT 19 February (Fig. 29) a surface cyclone with a central contour value of 1024 mb is located east of Maryland, slightly north of the observed cyclone's position. Only weak troughing is present above and to the west of the surface low at the 850 mb and 500 mb levels.

c. Analysis of cyclogenetic forcing

Examination of the GLAS model forecasts presented in this section shows that substantial differences in the prediction of cyclogenesis resulted from the use of different initial conditions as well as the exclusion of sensible and latent heat fluxes. The results of these forecasts suggest that the major factors contributing to the intensity of cyclogenesis in this case were the heating of the atmosphere above the warm coastal waters adjacent to the east coast and the strong upper level trough moving toward this area.

To further understand the role of these processes, we present in Figs. 30-33 vertical cross sections of temperature, absolute vorticity, vorticity advection, and divergence along latitute 38° N for the four 36 h GLAS model forecasts from 0000 GMT 18 Febraury 1979. Comparison of the forecasts with and without surface sensible heat and/or moisture fluxes (Figs. 30 - 32) shows the role of these fluxes in contributing to the generation of low level cyclonic vorticity and upper level anticyclonic vorticity from 70-75° W. Significant diabatic heating resulting from these fluxes is evident from the surface to 500 mb. As a result, the upper-level gradient of vorticity, vorticity advection, and divergence, and low level vorticity production by convergence are greatly increased in advance of the upper level trough.

Comparison of the forecasts from the GLAS and NMC analyses (Figs. 30 and 33) as well as the forecast from 0000 GMT 16 February (not shown) shows the importance of the intensity of the upper-level trough and to a lesser extent the intensity of diabatic heating to the predicted cyclogenesis. The result of the weaker upper-level trough and slightly weaker diabatic heating in the forecast from the interpolated NMC analysis is also to give a weaker upper-level gradient of vorticity, vorticity advection, and divergence and hence less cyclonic development at the surface.

5. CONCLUSIONS

On 18-19 February 1979, an intense cyclone developed along the east coast of the United States and produced very heavy snowfall from Virginia to southeast New York. The Barotropic model in use at the National Meteorolgical Center did not provide any indication of strong upper-air forcing for this storm, while the Seven-Level Primitive Equation Model and LFM-II greatly underestimated the strong positive vorticity advection along the east coast on 19 February as well as the surface cyclogenesis.

A series of forecast experiments was conducted to assess the accuracy of of the GLAS model's prediction of this storm and the importance of large-scale dynamical processes and diabatic heating to the cyclogenesis. The GLAS model forecast from the GLAS analysis at 0000 GMT 18 February correctly predicted intense coastal cyclogenesis and heavy precipitation. An extended-range forecast from 0000 GMT 16 February as well as a forecast from the NMC analysis interpolated to the GLAS grid predicted only weak coastal low development. A forecast with surface heat and moisture fluxes eliminated failed to predict any cyclogenesis while a similar forecast with only the surface moisture flux excluded showed weak development. Detailed examination of these forecasts shows that diabatic heating resulting from oceanic fluxes significantly contributed to the generation of low level cyclonic vorticity and the intensification and slow rate of movement of an upper level ridge over the western Atlantic. As an upper level short-wave trough approached this ridge, diabatic heating associated with the release of latent heat intensified and the gradient of vorticity, vorticity advection and upper level divergence in advance of the trough were greatly increased, providing strong large-scale forcing for the surface cyclogenesis and heavy precipitation.

In attempting to explain the intense cyclone development that occurred on 19 February and the reasons for the poor NMC model predictions, Bosart (1981) and Uccellini et al. (1981) emphasized subsynoptic processes and the interaction of synoptic and subsynoptic scales. However the GLAS model forecast from 0000 GMT 18 February which included sensible and latent heat fluxes was remarkably accurate in its prediction of cyclogenesis on 19 February and the subsequent movement and further intensification of this storm, even though it could not resolve either the coastal front discussed by Bosart, or the magnitude of the jet streak processes discussed by Uccellini et al. It is clearly not possible to study the specific effects of subsynoptic processes on the observed cyclone development with a coarse model and such effects probably did play a role in the details of the storm's evolution. The results presented here indicate, however, that strong large-scale forcing for cyclogenesis was present in this case. The model's simulation of this forcing and its parameterization of subgrid scale processes seemed sufficient to make an accurate prediction of the storm.

ACKNOWLEDGEMENT

The work presented in this paper is an outgrowth of experiments with the second-order GLAS model which were presented by W. Baker and R. Atlas at the Second Extratropical Cyclone Project Workshop. The authors benefitted from discussions with L. Uccellini and other attendees of that workshop as well as from discussions with D. Atlas, W. Baker, M. Ghil, M. Halem, E. Kalnay, and Y. Sud. We gratefully acknowledge D. Edelmann and C. Long for providing computing and graphics support. M. Iredell and E. Kalnay for performing the model integrations with and without surface fluxes, L. Rumberg for drafting the figures, and J. Wentz for typing the manuscript.

REFERENCES

Baker, W., D. Edelmann, M. Iredell, D. Han, and S, Jakkempudi, 1981: Objective analysis of observational data from the FGGE observing systems. NASA Tech. Memo. 82062, [NTIS N8122623] 132 pp.

Bosart, L. F., 1981: The Presidents' Day snowstorm of 18-19 February 1979: A subsynoptic-scale event. Mon. Wea. Rev., 109, 1542-1566.

Cressman, G. P., 1959: An operational objective analysis system. Mon. Wea. Rev., 87, 367-374.

_____ , 1978: A notable forecasting achievement. Bull. Amer. Meteor. Soc., 59, 370.

Halem, M., E. Kalnay-Rivas, W. E. Baker, and R. Atlas, 1982: An assessment of the FGGE satellite observing system during SOP-1. Accepted by Bull. Amer. Meteor. Soc.

Kalnay-Rivas, E., A. Bayliss, and J. Storch, 1977: The 4th order GISS model of the global atmosphere. Beitr. Phys. Atmos., 50, 299-311.

Kalnay-Rivas, E., and D. Hoitsma, 1979: The effect of accuracy, conservation and filtering on numerical weather forecasting. Preprints Fourth Conf. on Numerical Weather Prediction, Silver Spring, Maryland, Amer. Meteor. Soc., 302-312.

Staff, National Weather Analysis Center, 1960: Synoptic Meteorology As Practiced by the National Meteorological Center. Washington, D. C., 35 pp.

Sud, Y., and J. Abeles, 1981: Calculation of surface temperature and surface fluxes in the GLAS GCM. NASA Tech. Memo. 82167.

Uccellini, L. W., P. J. Kocin, and C. H. Wash, 1981: The President's Day cyclone of 17-19 February 1979: An analysis of jet streak interaction prior to cyclogenesis. NASA Tech. Memo. 82077 59 pp. [NTIS N 81-20658]

Wu, M.-L. C., 1980: The exchange of infrared radiative energy in the troposphere. J. Geophys. Res., 85, 4084-4090.

Table 1 Description of Experiments

Experiment	Forecast Model	Initial Conditions
1	GLAS GCM	GLAS Analysis at 0000 GMT 18 Feb.
2	Same as 1 but without surface sensible heat and moisture fluxes	GLAS Analysis at 0000 GMT 18 Feb.
3	Same as 1 but without surface moisture flux	GLAS Analysis at 0000 GMT 18 Feb.
4	Same as 1	NMC Analysis at 0000 GMT 18 Feb.
5	Same as 1	GLAS Analysis at 0000 GMT 16 Feb.

FIGURE CAPTIONS

Fig. 1 National Weather Service 500 mb (top) 850 mb (middle) and surface (bottom) analyses for 0000 GMT 18 February 1979.

Fig. 2 Same as Fig. 1 for 1200 GMT 18 February 1979.

Fig. 3 Same as Fig. 1 for 0000 GMT 19 February 1979.

Fig. 4 Same as Fig. 1 for 1200 GMT 19 February 1979.

Fig. 5 Same as Fig. 1 for 0000 GMT 20 February 1979.

Fig. 6 Barotropic model 0000 GMT 18 February 1979 analysis (top), 36 h forecast valid at 1200 GMT 19 February 1979 (middle), and 1200 GMT 19 February 1979 (bottom) analysis of 500 mb geopotential height (solid lines) and absolute vorticity (dashed lines).

Fig. 7 Sea-level pressure analysis and LFM-II 12 h, 24 h, and 36 h sea-level pressure (solid lines) and 1000-500 mb thickness (dashed lines) forecasts valid at 1200 GMT 19 February 1979 (after Uccellini et al., 1981).

Fig. 8 Same as Fig. 7 for 500 mb geopotential height and absolute vorticity.

Fig. 9 GLAS analysis of 500 mb geopotential height and temperature (top) 850 mb geopotential height and temperature (middle), and sea-level pressure and 1000-500 mb thickness (bottom) at 0000 GMT 18 February 1979.

Fig. 10 Same as Fig. 9 for NMC analysis interpolated to the GLAS grid.

Fig. 11 Same as Fig. 9 for 12 h GLAS model forecast from the GLAS analysis at 0000 GMT 18 February 1979.

Fig. 12 Same as Fig. 9 for 24 h GLAS model forecast from the GLAS analysis at 0000 GMT 18 February 1979.

Fig. 13 Same as Fig. 9 for 36 h GLAS model forecast from the GLAS analysis at 0000 GMT 18 February 1979.

Fig. 14 Same as Fig. 9 for 48 h GLAS model forecast from the GLAS analysis at 0000 GMT 18 February 1979.

Fig. 15 Same as Fig. 9 for 12 h GLAS model forecast without surface heat and moisture fluxes, from the GLAS analysis at 0000 GMT 18 February 1979.

Fig. 16 Same as Fig. 9 for 24 h GLAS model forecast without surface heat and moisture fluxes, from the GLAS analysis at 0000 GMT 18 February 1979.

Fig. 17 Same as Fig. 9 for 36 h GLAS model forecast without surface heat and moisture fluxes, from the GLAS analysis at 0000 GMT 18 February 1979.

Fig. 18 Same as Fig. 9 for 48 h GLAS model forecast without surface heat and moisture fluxes, from the GLAS analysis at 0000 GMT 18 February 1979.

Fig. 19 Same as Fig. 9 for 12 h GLAS model forecast without surface moisture flux from the GLAS analysis at 0000 GMT 18 February 1979.

Fig. 20 Same as Fig. 9 for 24 h GLAS model forecast without surface moisture flux from the GLAS analysis at 0000 GMT 18 February 1979.

Fig. 21 Same as Fig. 9 for 36 h GLAS model forecast without surface moisture flux from the GLAS analysis at 0000 GMT 18 February 1979.

Fig. 22 Same as Fig. 9 for 48 h GLAS model forecast without surface moisture flux from the GLAS analysis at 0000 GMT 18 February 1979.

Fig. 23 Same as Fig. 9 for 12 h GLAS model forecast from the NMC analysis at 0000 GMT 18 February 1979.

Fig. 24 Same as Fig. 9 for 24 h GLAS model forecast from the NMC analysis at 0000 GMT 18 February 1979.

Fig. 25 Same as Fig. 9 for 36 h GLAS model forecast from the NMC analysis at 0000 GMT 18 February 1979.

Fig. 26 Same as Fig. 9 for 48 h GLAS model forecast from the GLAS analysis at 0000 16 February 1979.

Fig. 27 Same as Fig. 9 for 60 h GLAS model forecast from the GLAS analysis at 0000 GMT 16 February 1979.

Fig. 28 Same as Fig. 9 for 72 h GLAS model forecast from the GLAS analysis at 0000 GMT 16 February 1979.

Fig. 29 Same as Fig. 9 for 84 h GLAS model forecast from the GLAS analysis at 0000 GMT 18 February 1979.

Fig. 30 Vertical cross sections of temperature, absolute vorticity, vorticity advection, and divergence along latitude 38° N for the 36 h GLAS model forecast from the GLAS analysis at 0000 GMT 18 February 1979.

Fig. 31 Same as Fig. 30 for 36 h forecast without surface sensible heat and moisture fluxes.

Fig. 32 Same as Fig. 30 for 36 h forecast without surface evaporation.

Fig. 33 Same as Fig. 30 for 36 h forecast from the NMC analysis.

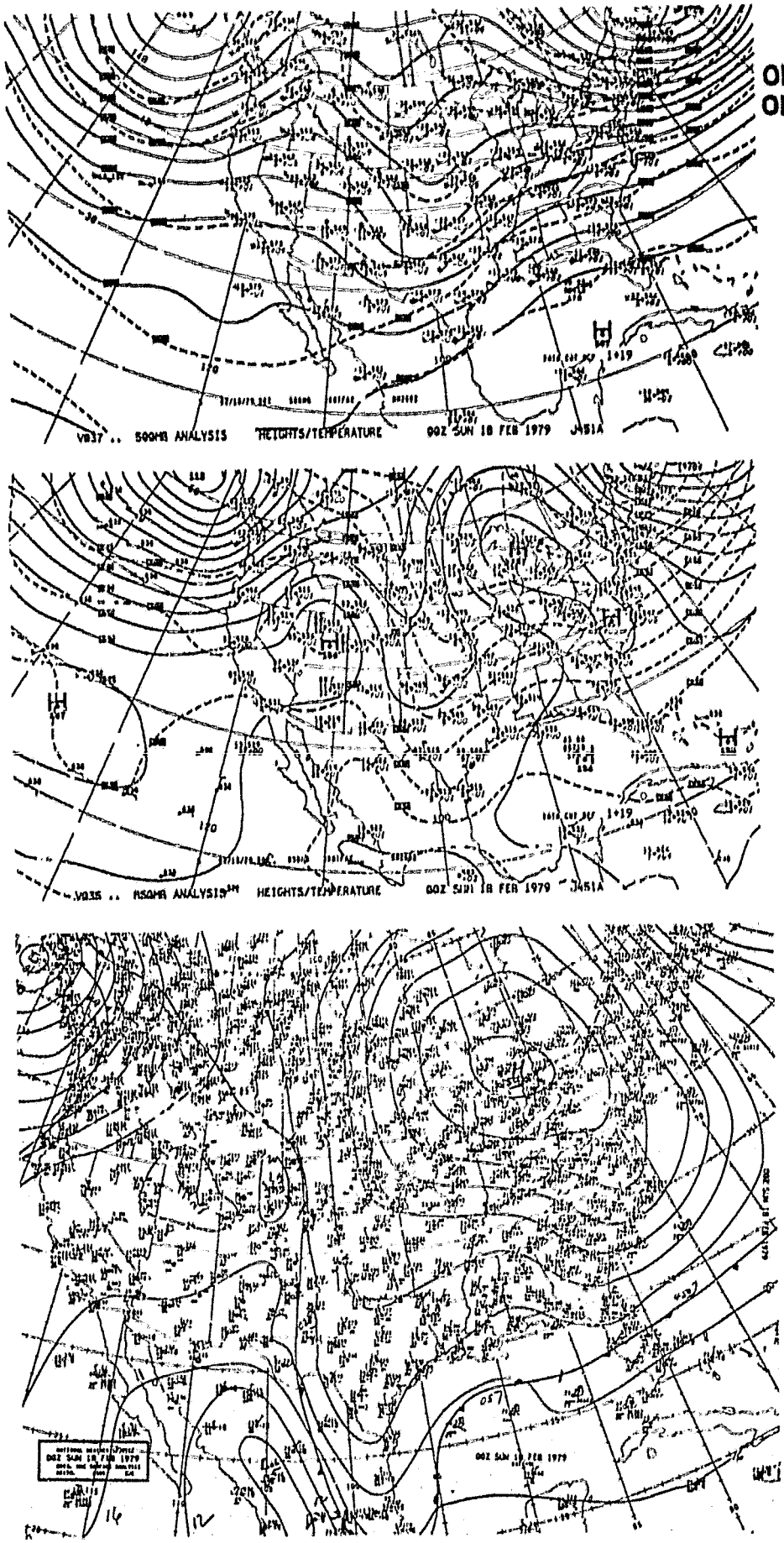

Fig. 1 National Weather Service 500 mb (top) 850 mb (middle) and surface (bottom) analyses for 0000 GMT 18 February 1979.

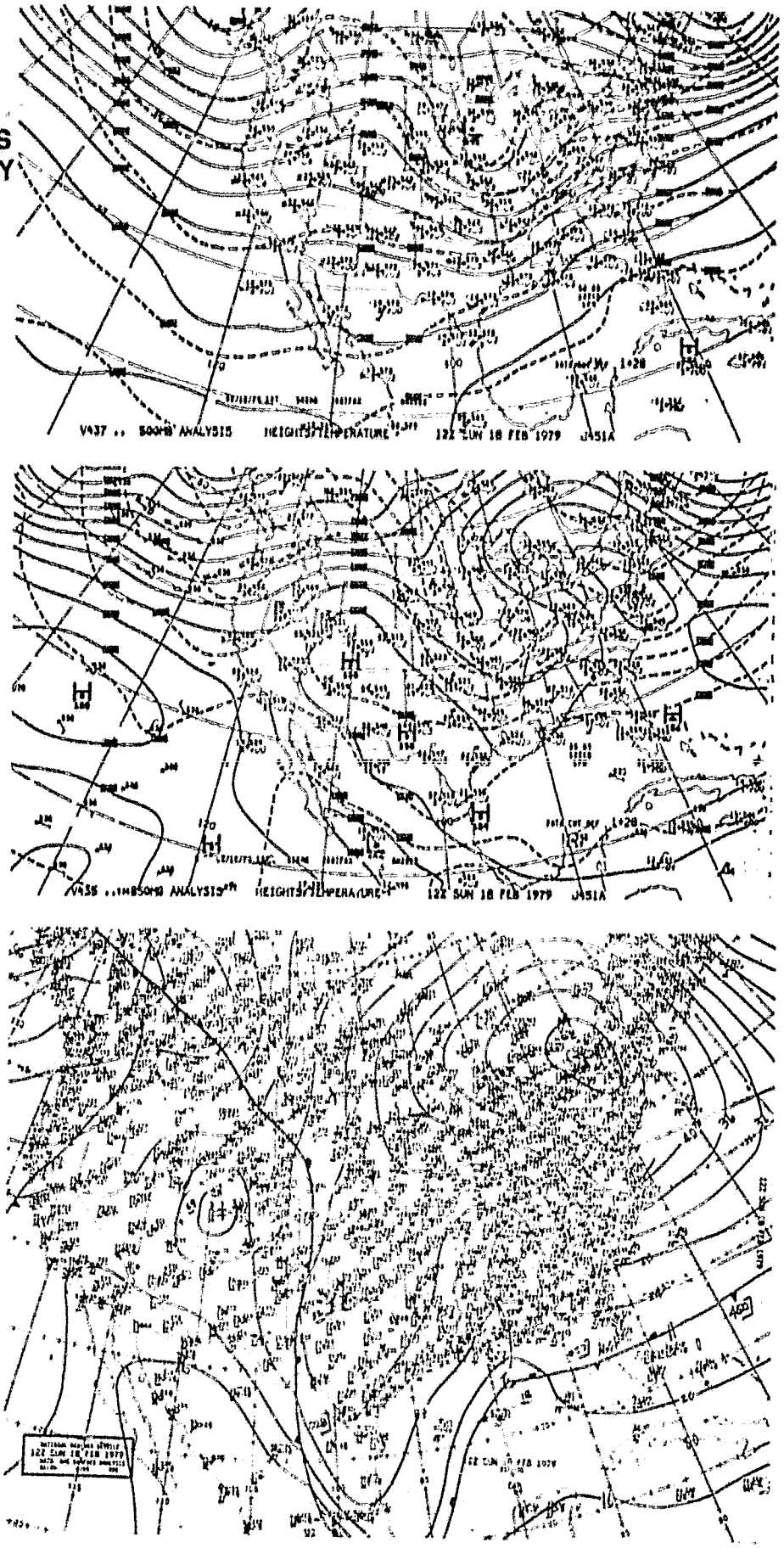

Fig. 2 Same as Fig. 1 for 1200 GMT 18 February 1979.

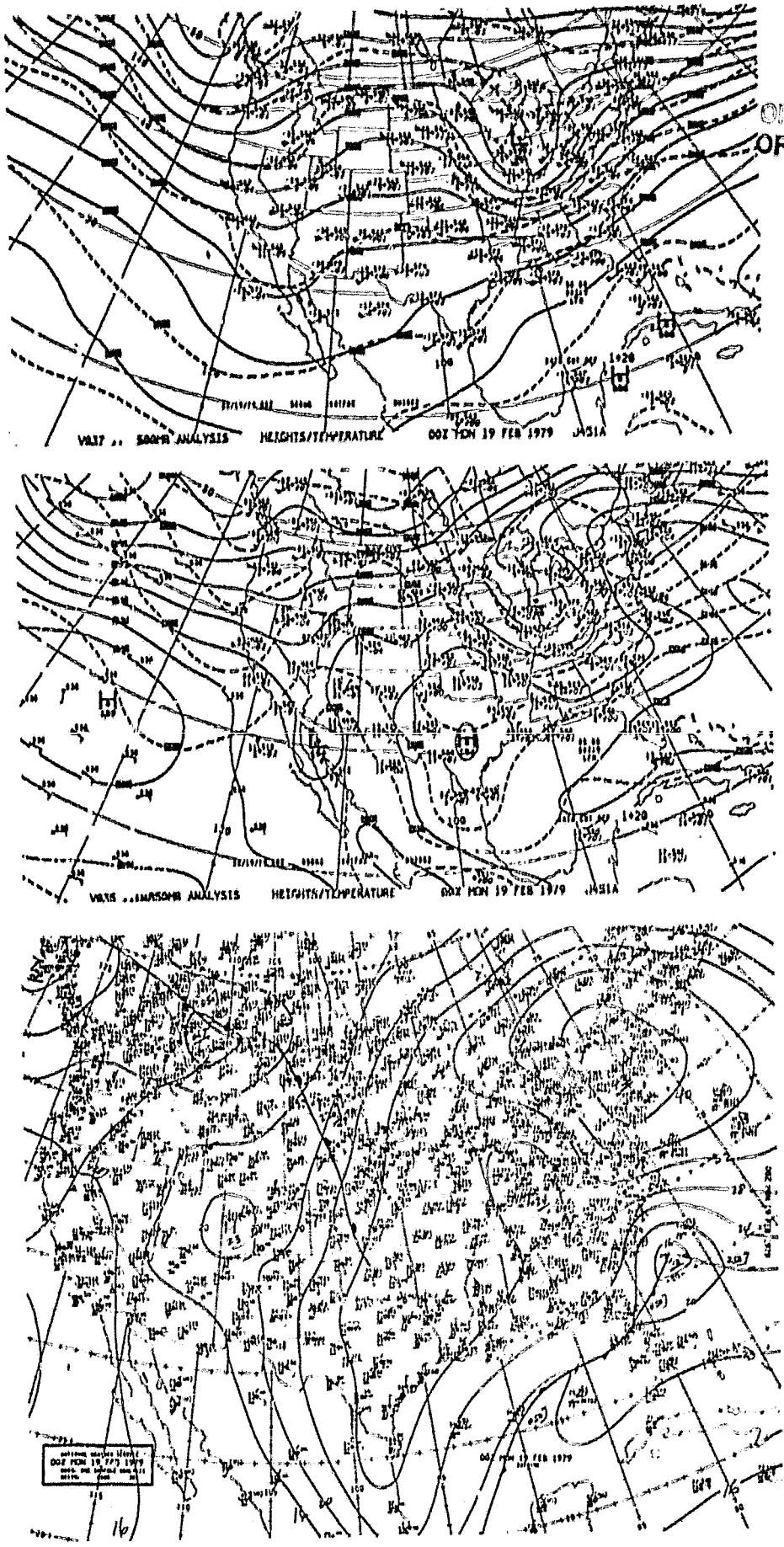

Fig. 3 Same as Fig. 1 for 0000 GMT 19 February 1979.

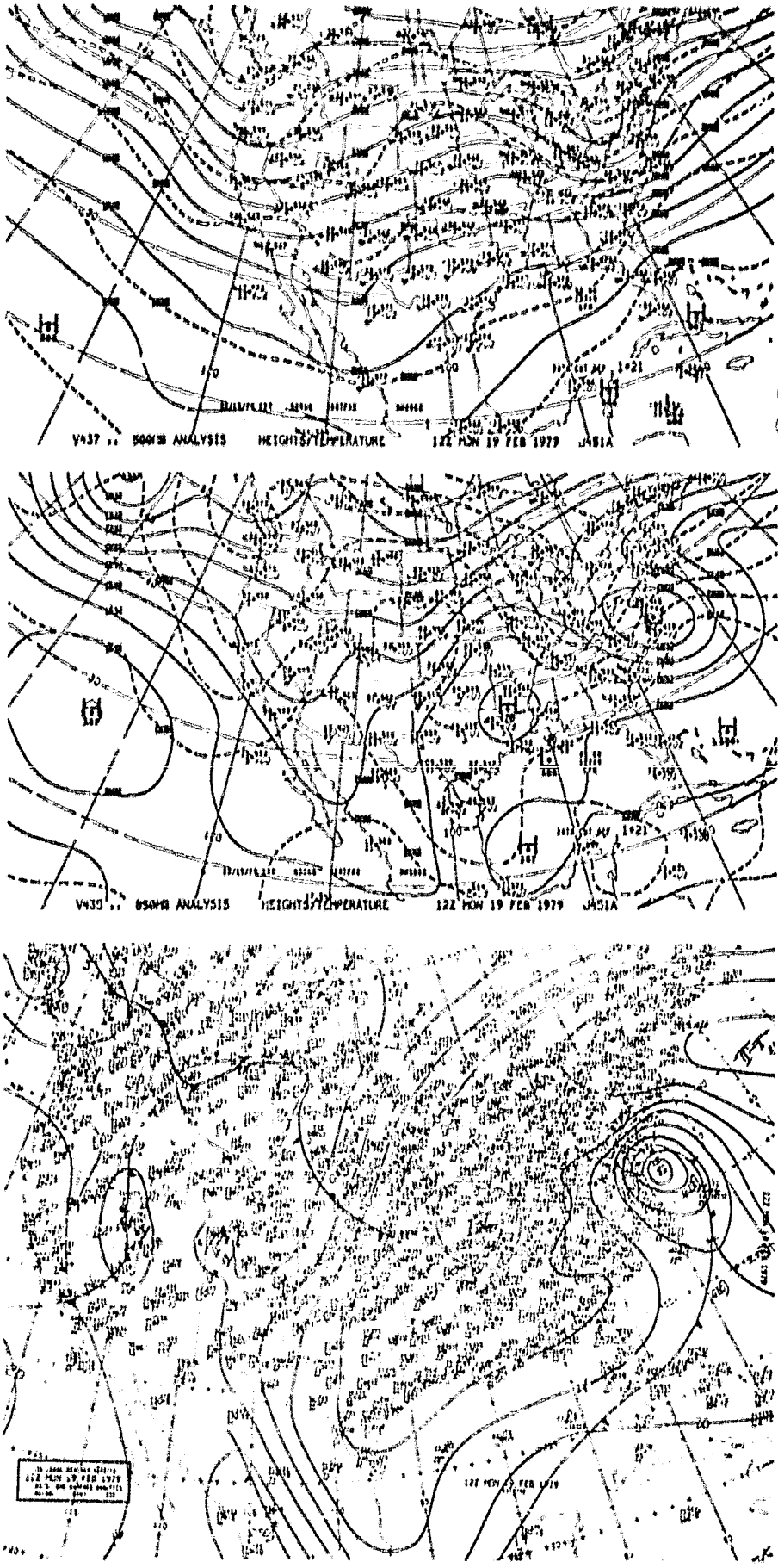

Fig. 4 Same as Fig. 1 for 1200 GMT 19 February 1979.

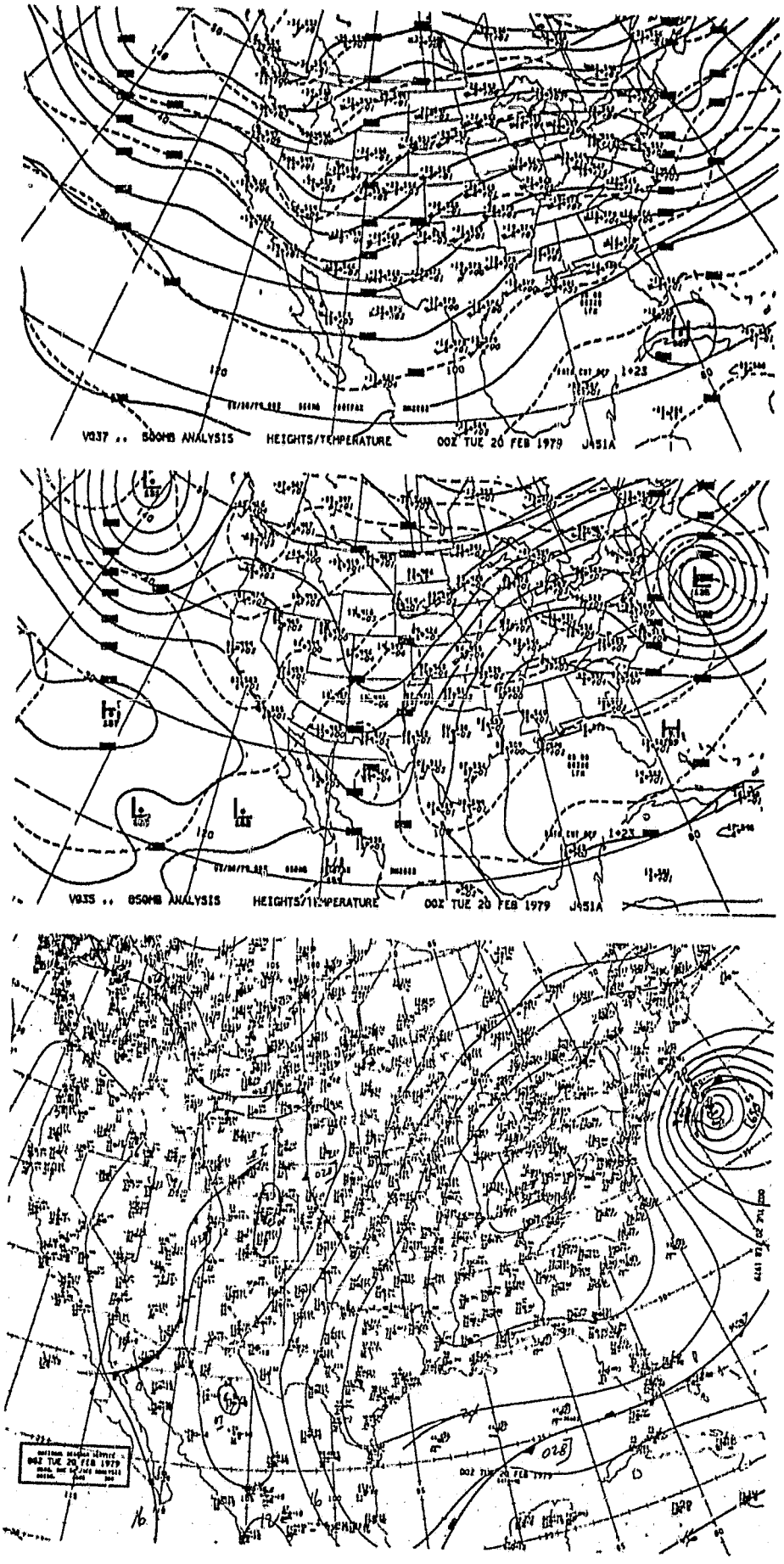

Fig. 5 Same as Fig. 1 for 0000 GMT 20 February 1979.

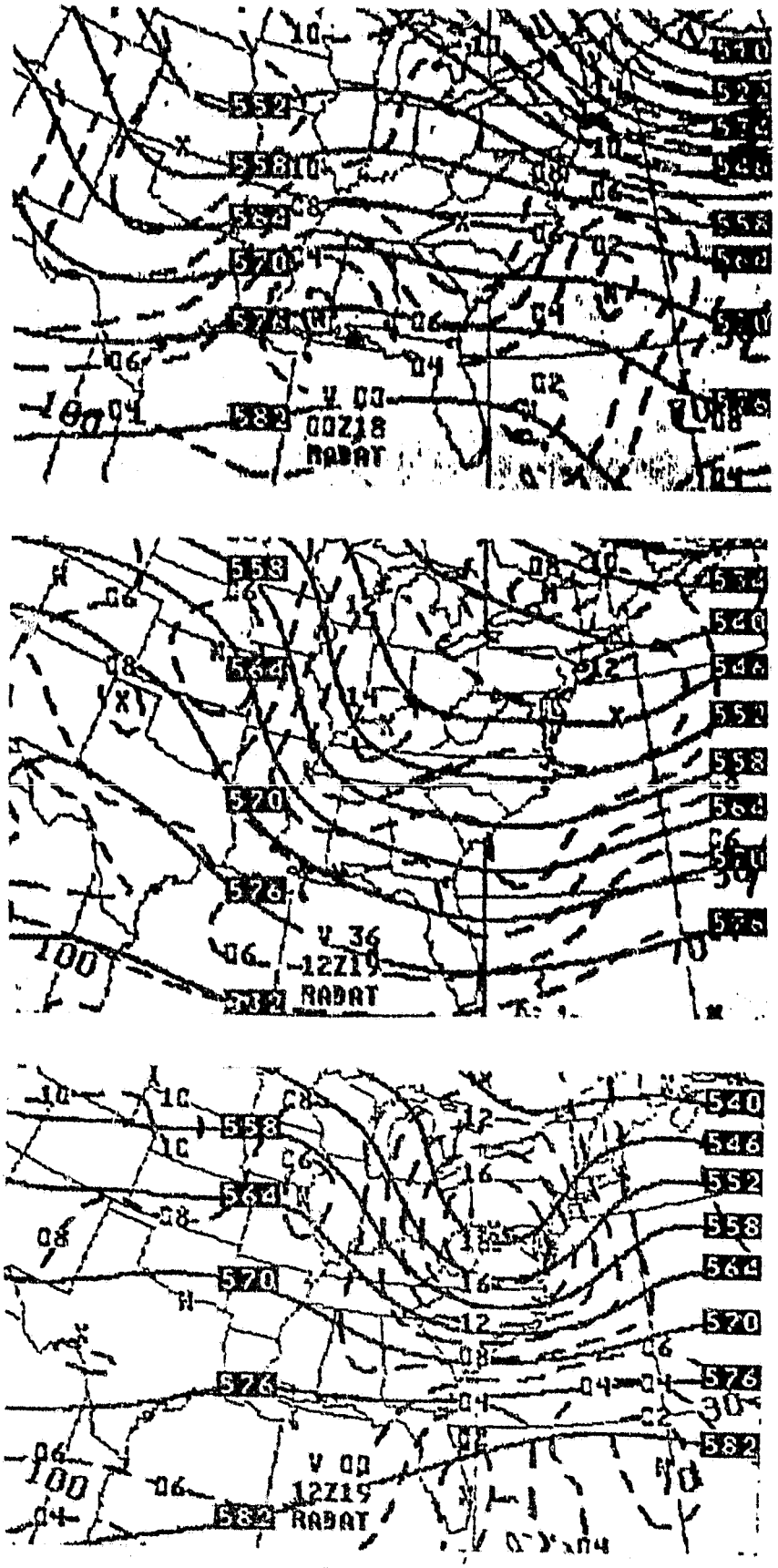

Fig. 6 Barotropic model 0000 GMT 18 February 1979 analysis (top), 36 h forecast valid at 1200 GMT 19 February 1979 (middle), and 1200 GMT 19 February 1979 (bottom) analysis of 500 mb geopotential height (solid lines) and absolute vorticity (dashed lines).

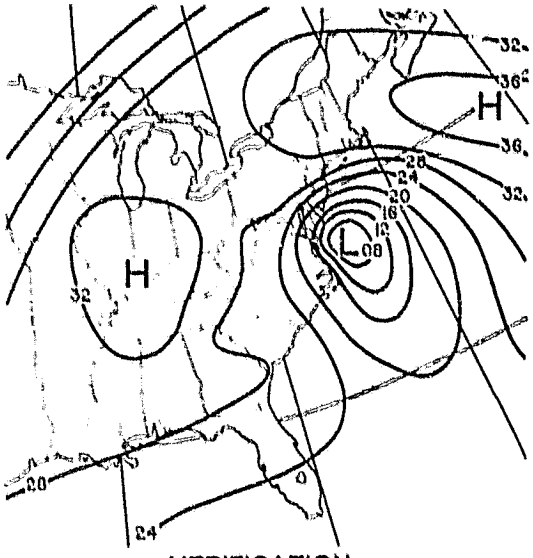

VERIFICATION

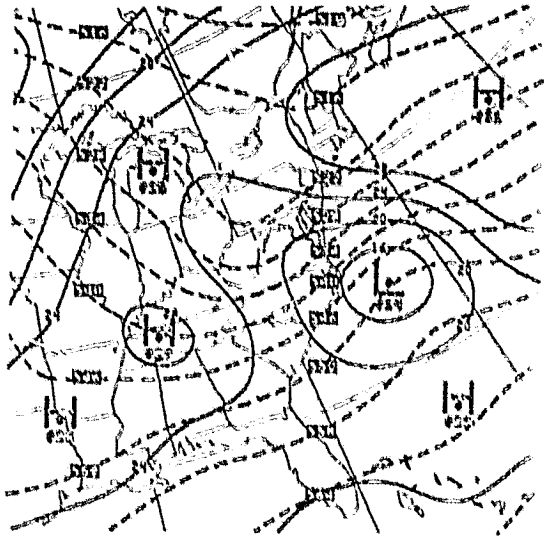

12 HR FORECAST INITIALIZED AT
0000 GMT 19 FEB 1979

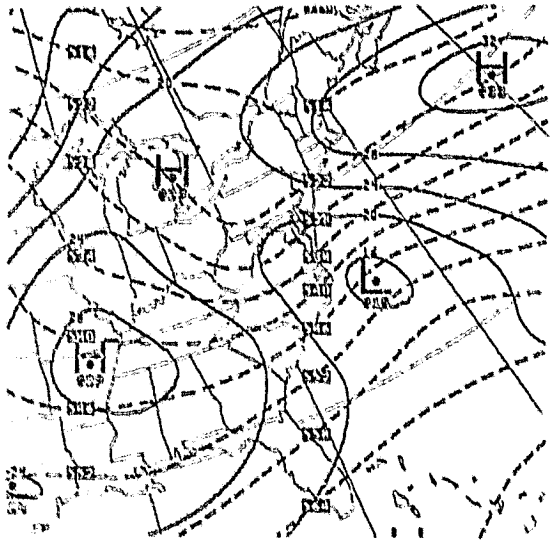

24 HR FORECAST INITIALIZED AT
1200 GMT 18 FEB 1979

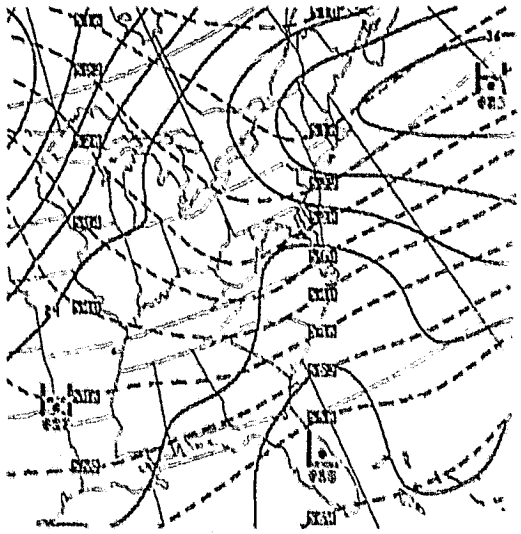

36 HR FORECAST INITIALIZED AT
0000 GMT 18 FEB 1979

Fig. 7 Sea-level pressure analysis and LFM-II 12 h, 24 h, and 36 h sea-level pressure (solid lines) and 1000-500 mb thickness (dashed lines) forecasts valid at 1200 GMT 19 February 1979 (after Uccellini et al., 1981).

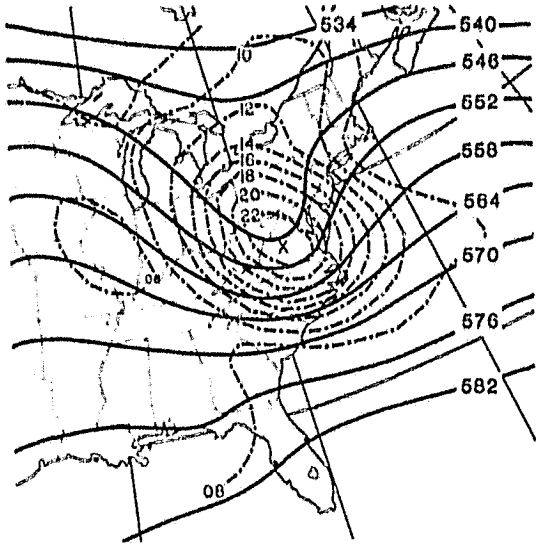

VERIFICATION

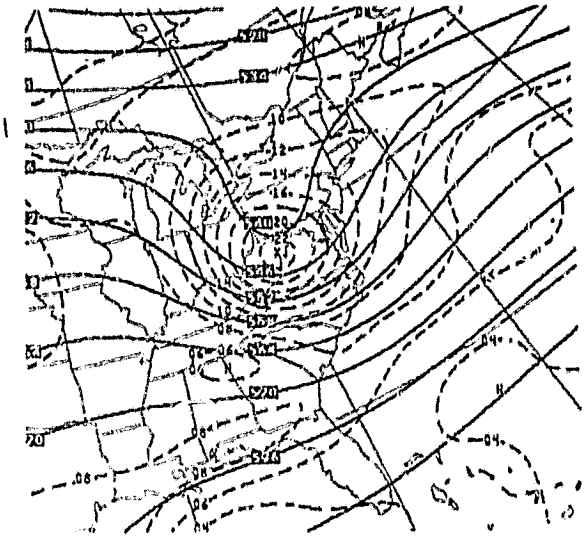

12 HR FORECAST INITIALIZED AT
0000 GMT 19 FEB 1979

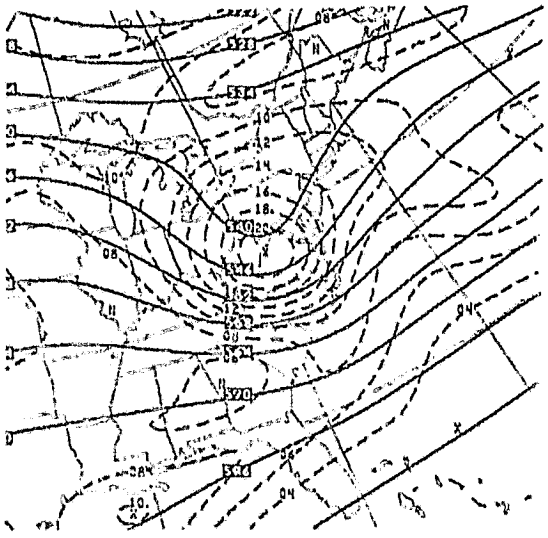

24 HR FORECAST INITIALIZED AT
1200 GMT 18 FEB 1979

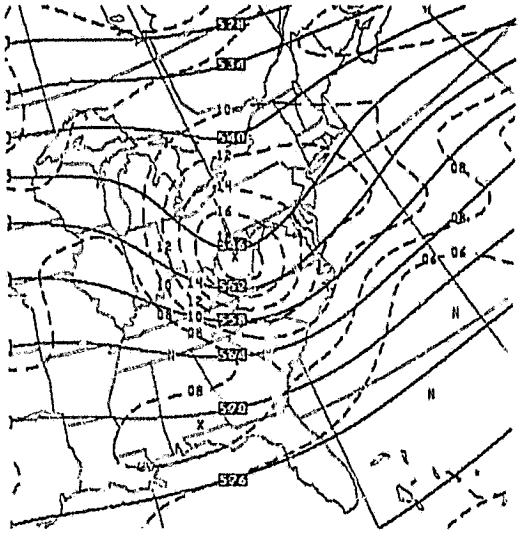

36 HR FORECAST INITIALIZED AT
0000 GMT 18 FEB 1979

Fig. 8 Same as Fig. 7 for 500 mb geopotential height and absolute vorticity.

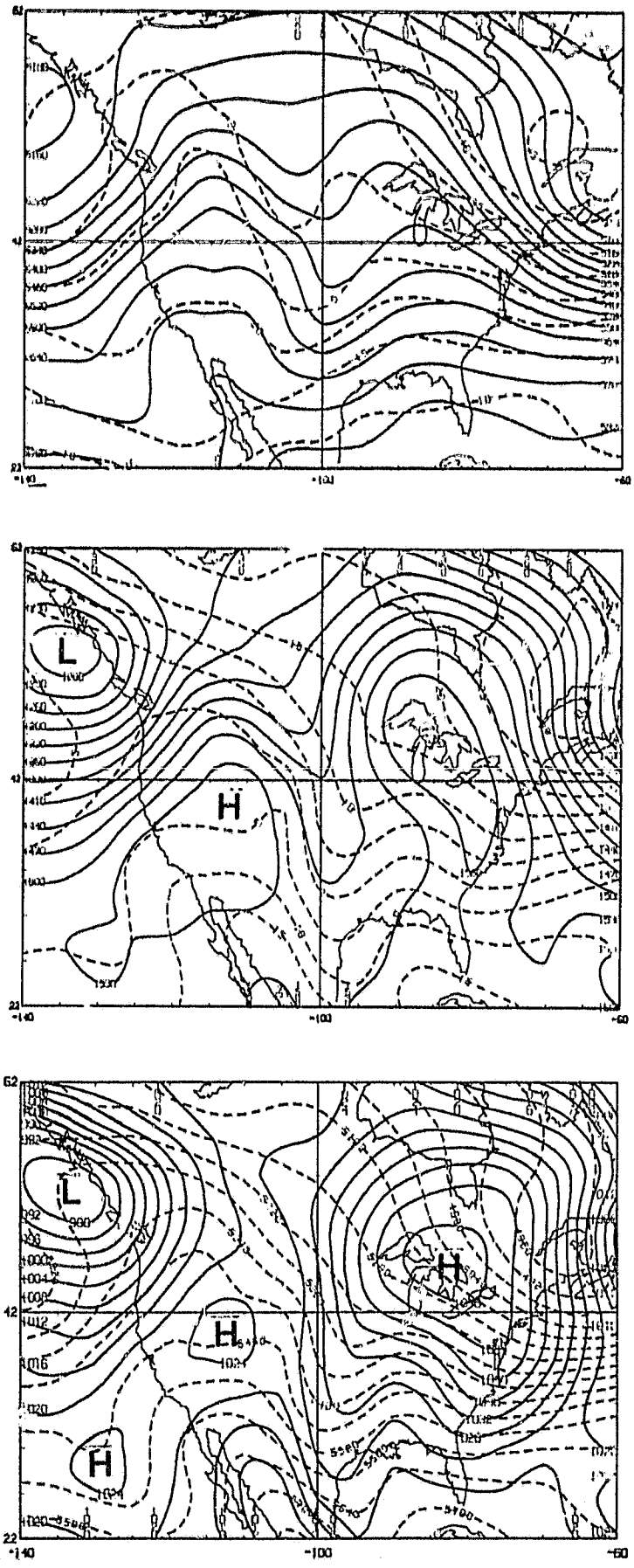

Fig. 9 GLAS analysis of 500 mb geopotential height and temperature (top) 850 mb geopotential height and temperature (middle), and sea-level pressure and 1000-500 mb thickness (bottom) at 0000 GMT 18 February 1979.

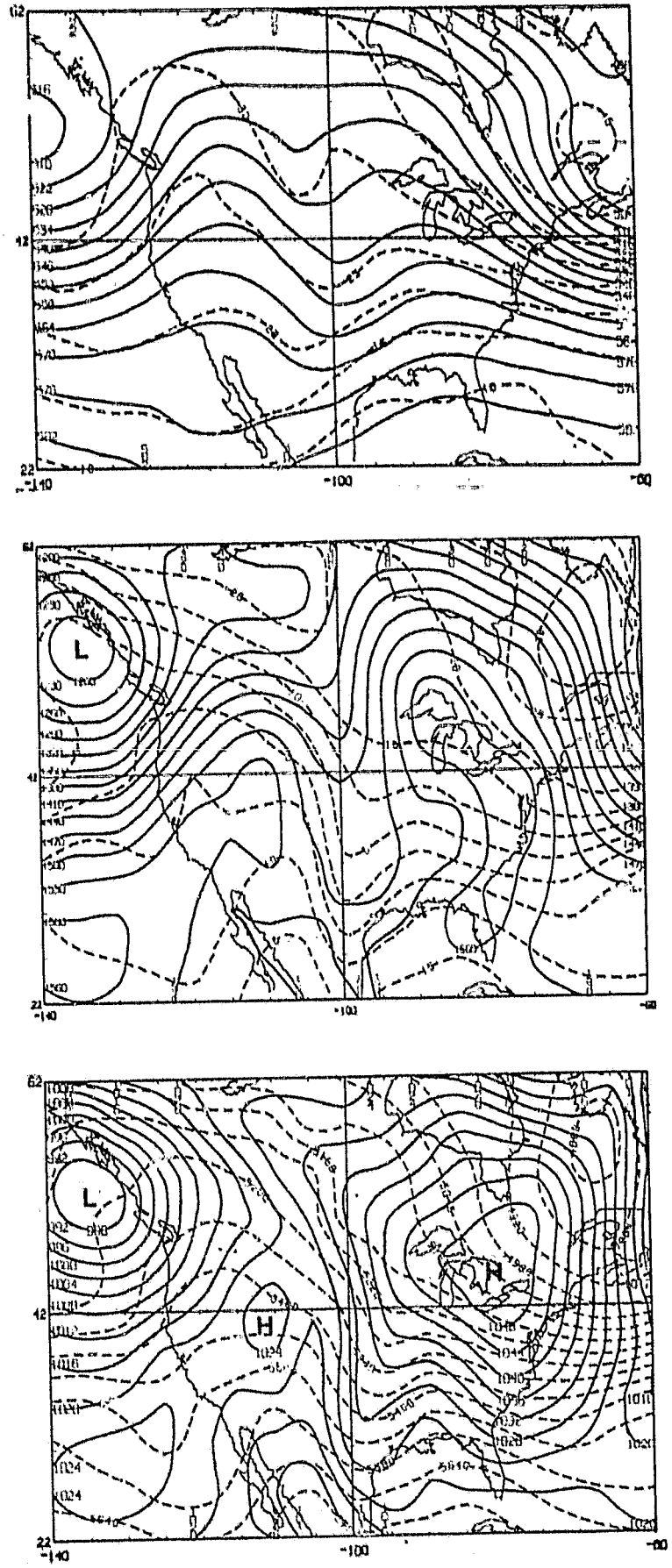

Fig. 10 Same as Fig. 9 for NMC analysis interpolated to the GLAS grid.

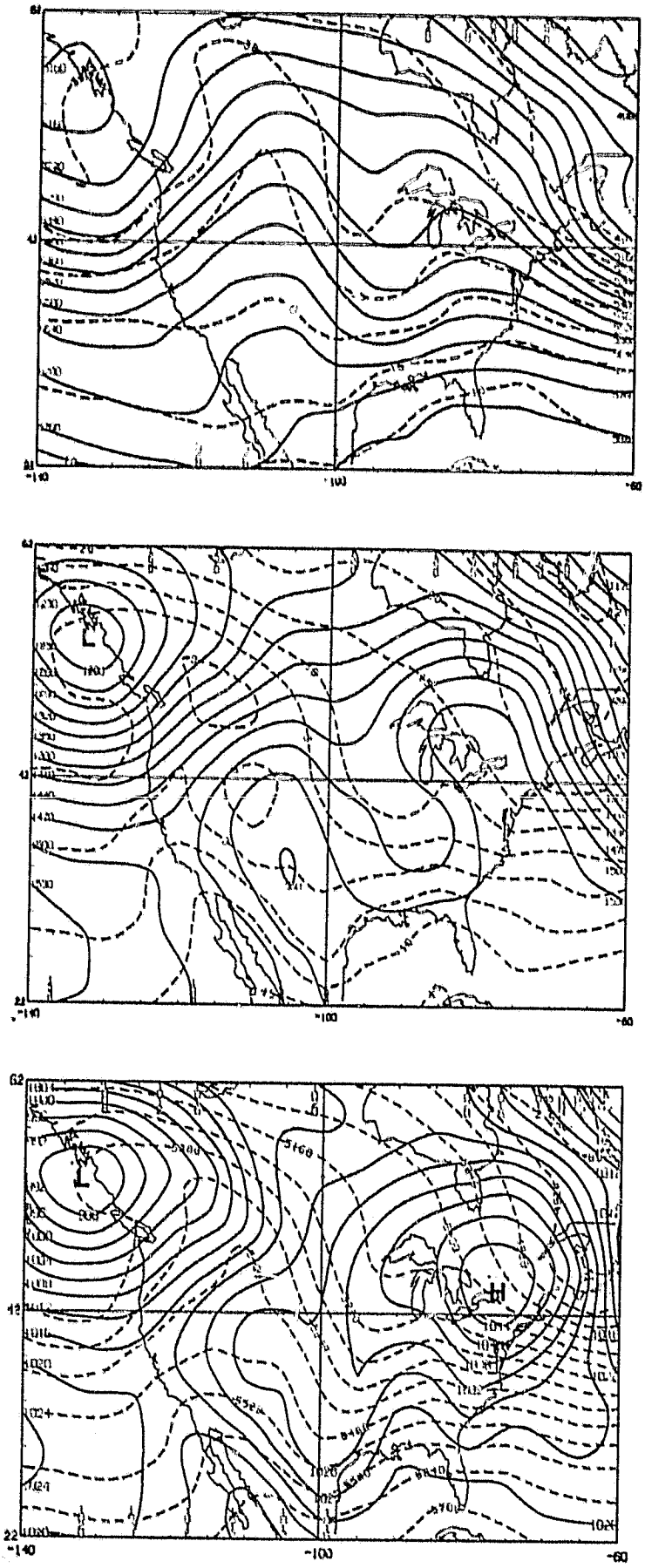

Fig. 11 Same as Fig. 9 for 12 h GLAS model forecast from the GLAS analysis at 0000 GMT 18 February 1979.

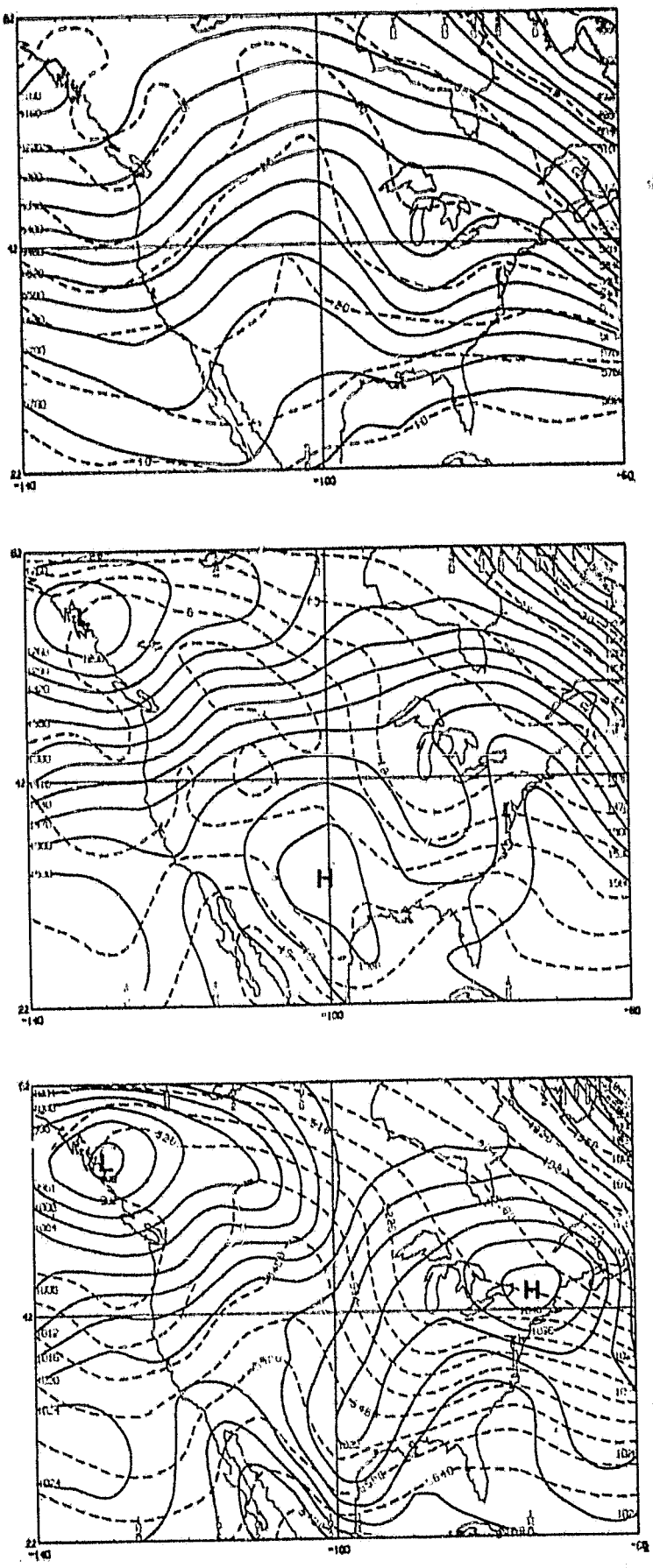

Fig. 12 Same as Fig. 9 for 24 h GLAS model forecast from the GLAS analysis at 0000 GMT 18 February 1979.

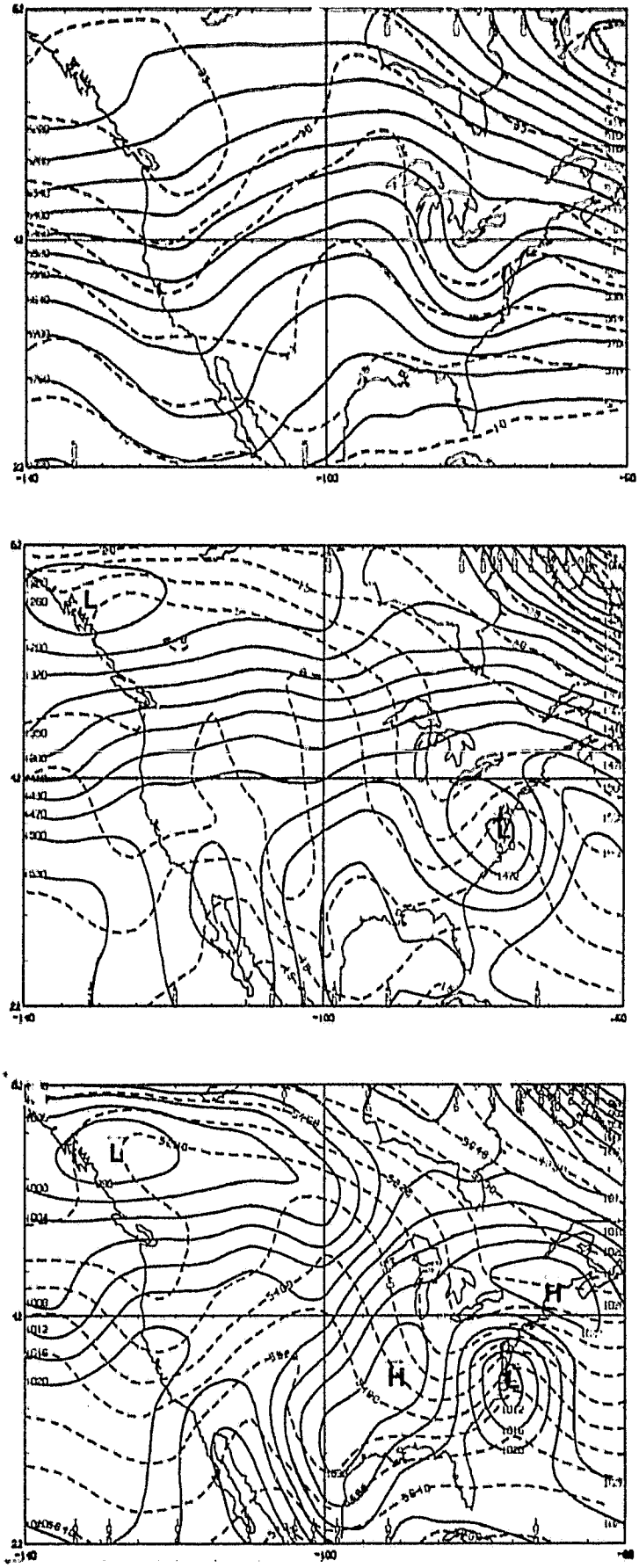

Fig. 13 Same as Fig. 9 for 36 h GLAS model forecast from the GLAS analysis at 0000 GMT 18 February 1979.

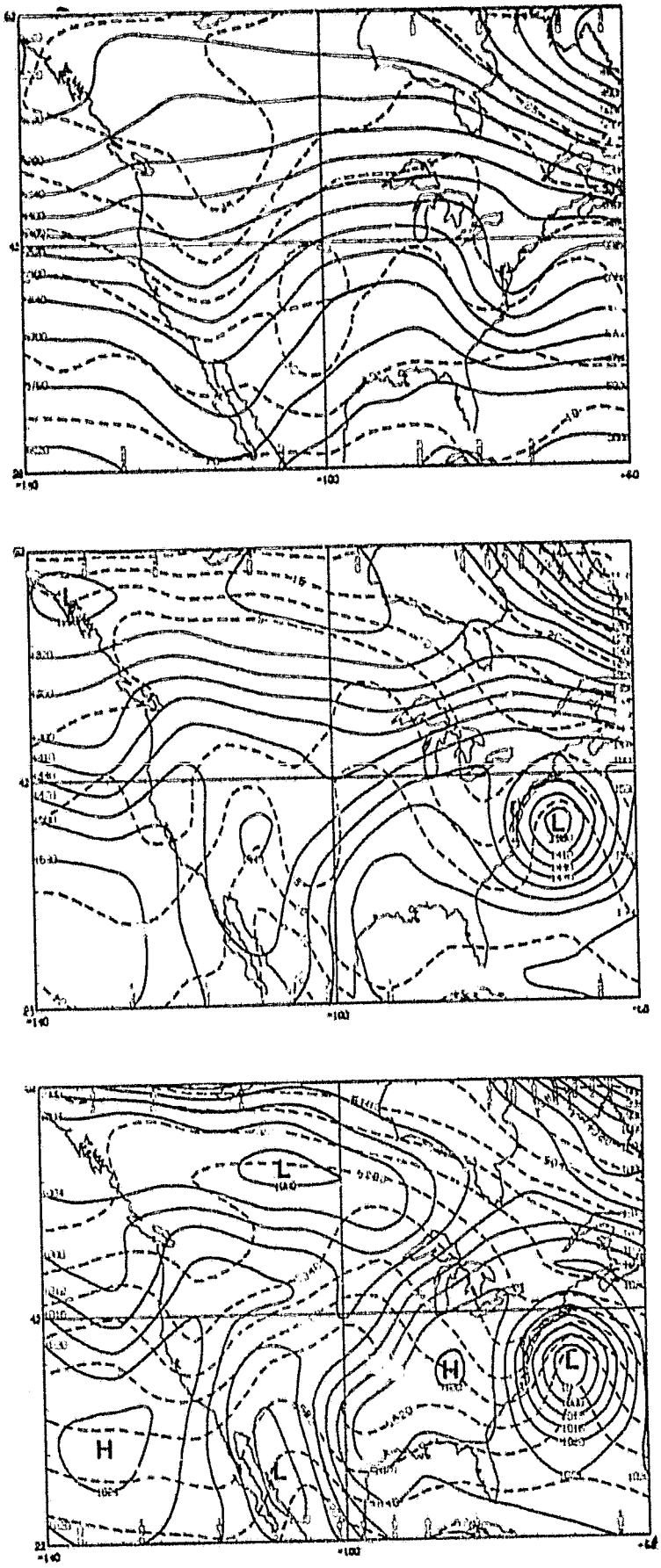

Fig. 14 Same as Fig. 9 for 48 h GLAS model forecast from the GLAS analysis at 0000 GMT 18 February 1979.

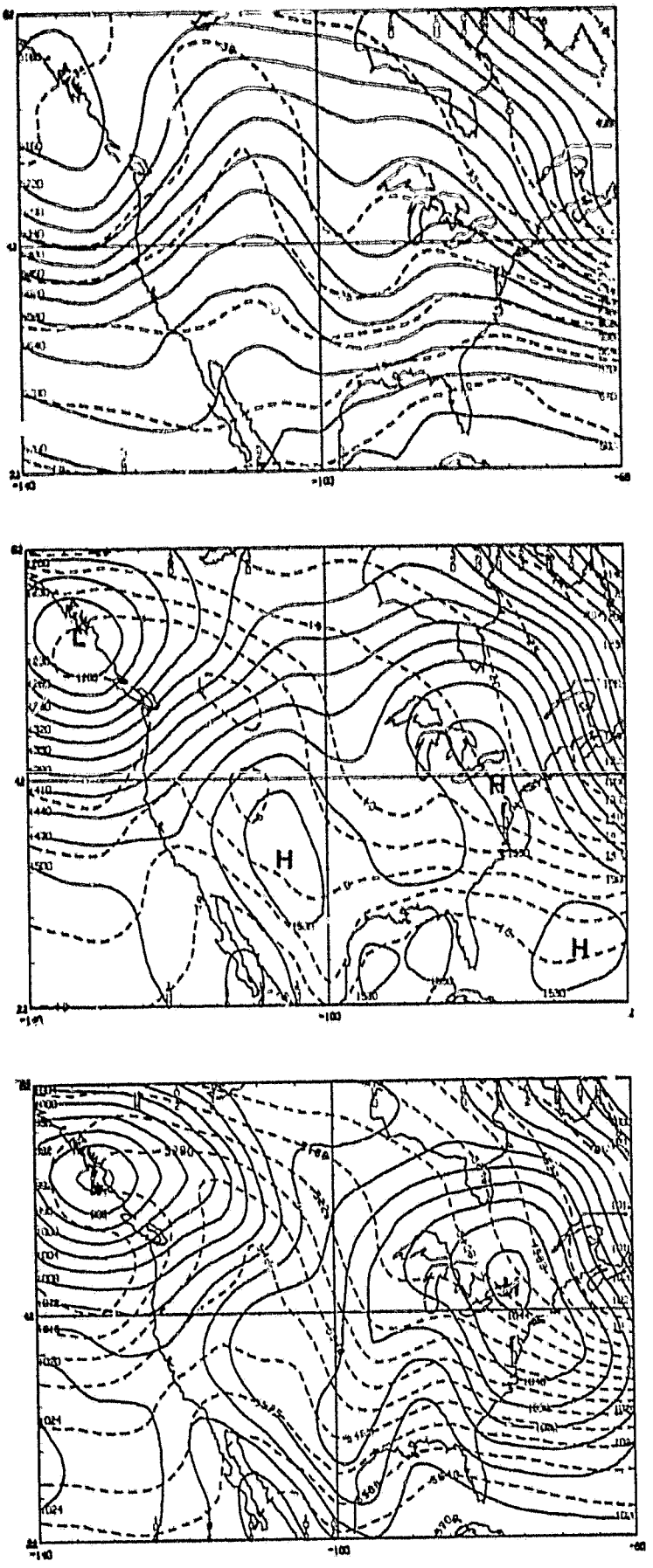

Fig. 15 Same as Fig. 9 for 12 h GLAS model forecast without surface heat and moisture fluxes, from the GLAS analysis at 0000 GMT 18 February 1979.

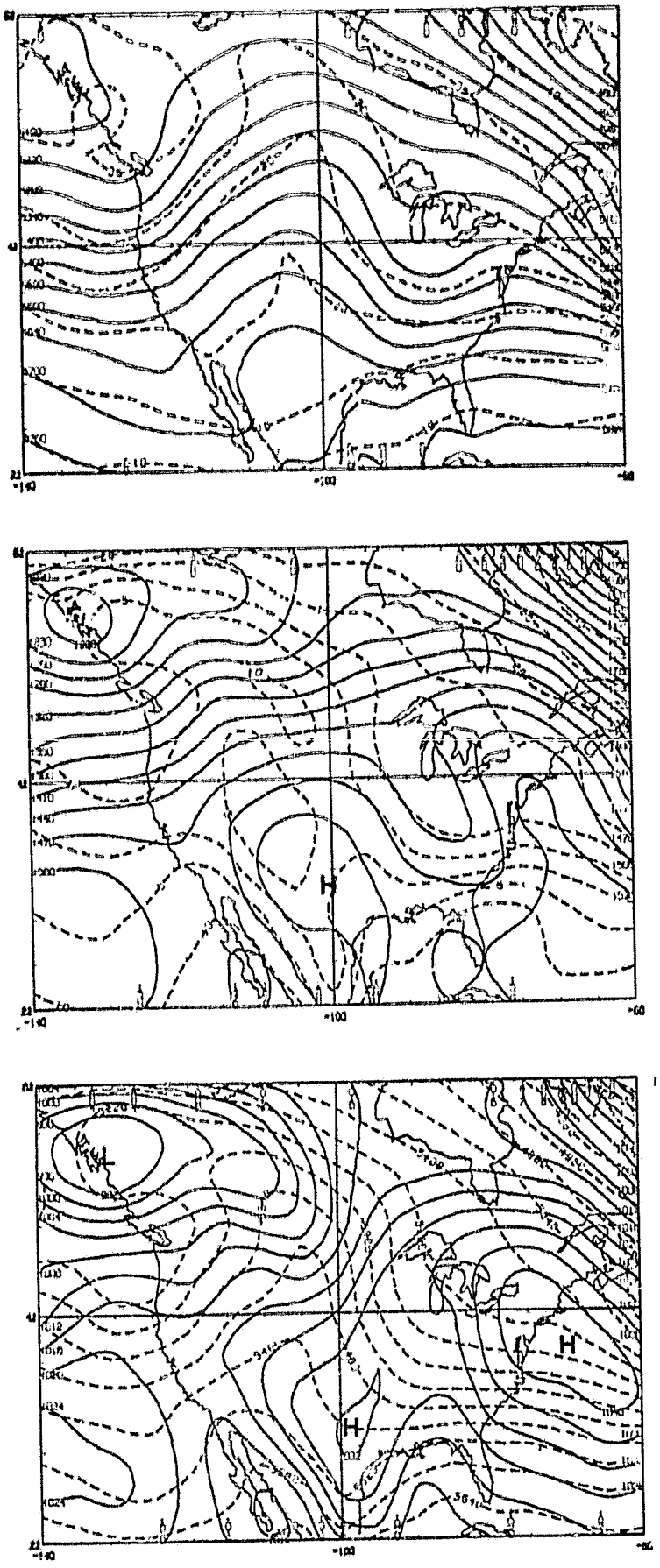

Fig. 16 Same as Fig. 9 for 24 h GLAS model forecast without surface heat and moisture fluxes, from the GLAS analysis at 0000 GMT 18 February 1979.

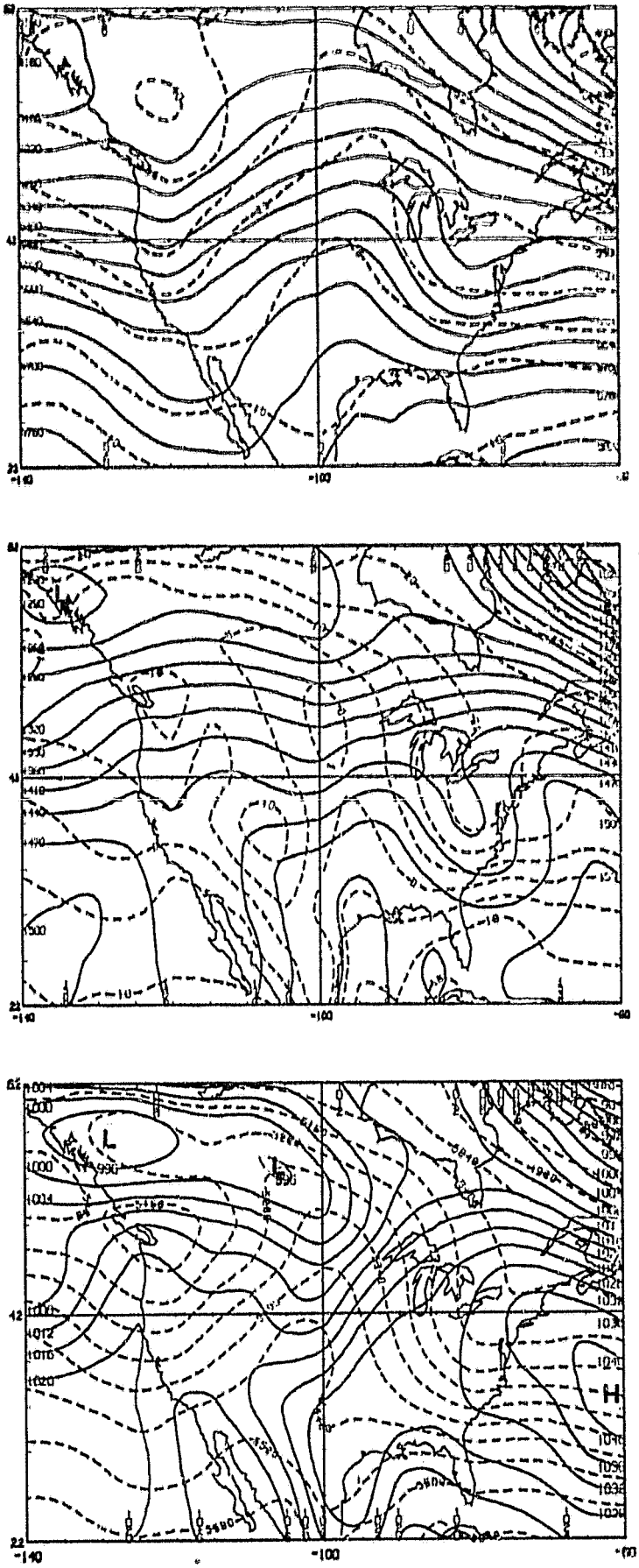

Fig. 17 Same as Fig. 9 for 36 h GLAS model forecast without surface heat and moisture fluxes, from the GLAS analysis at 0000 GMT 18 February 1979.

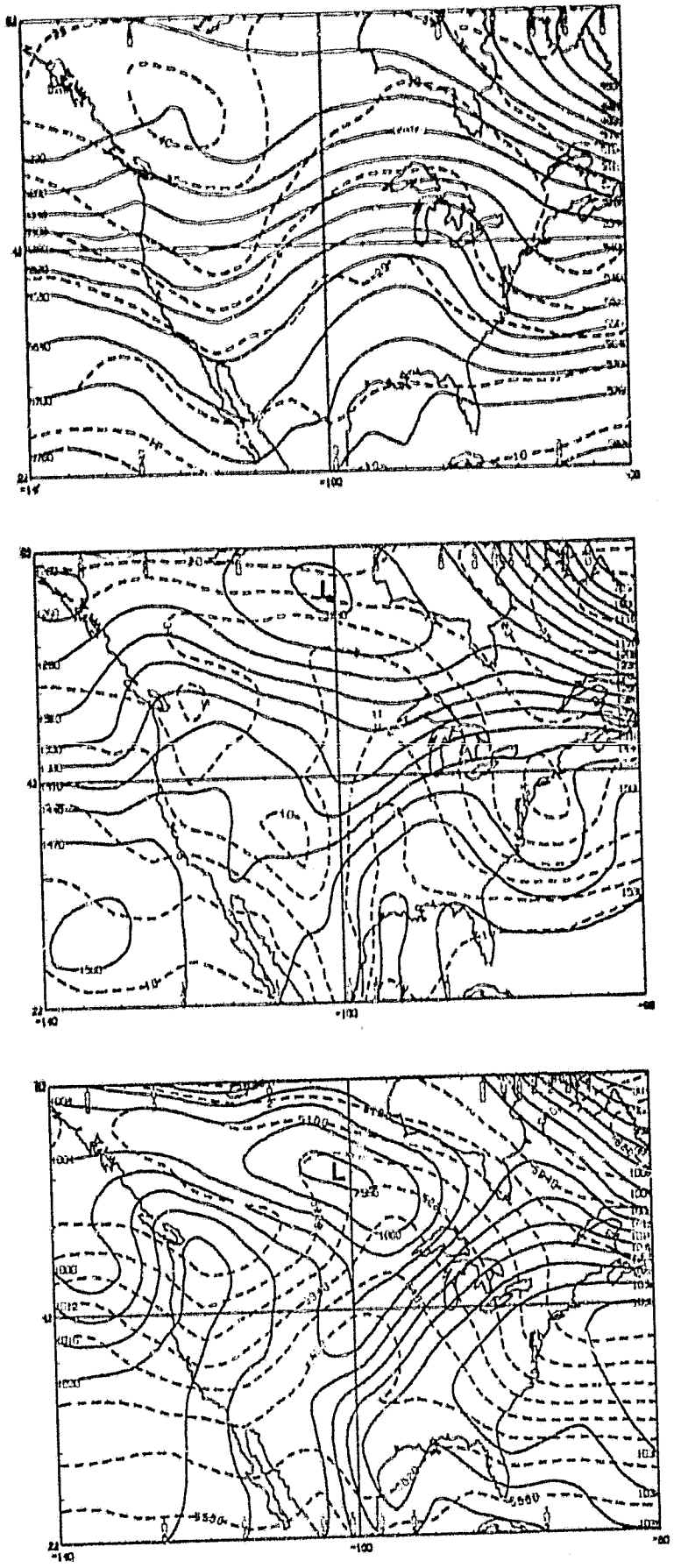

Fig. 18 Same as Fig. 9 for 48 h GLAS model forecast without surface heat and moisture fluxes, from the GLAS analysis at 0000 GMT 18 February 1979.

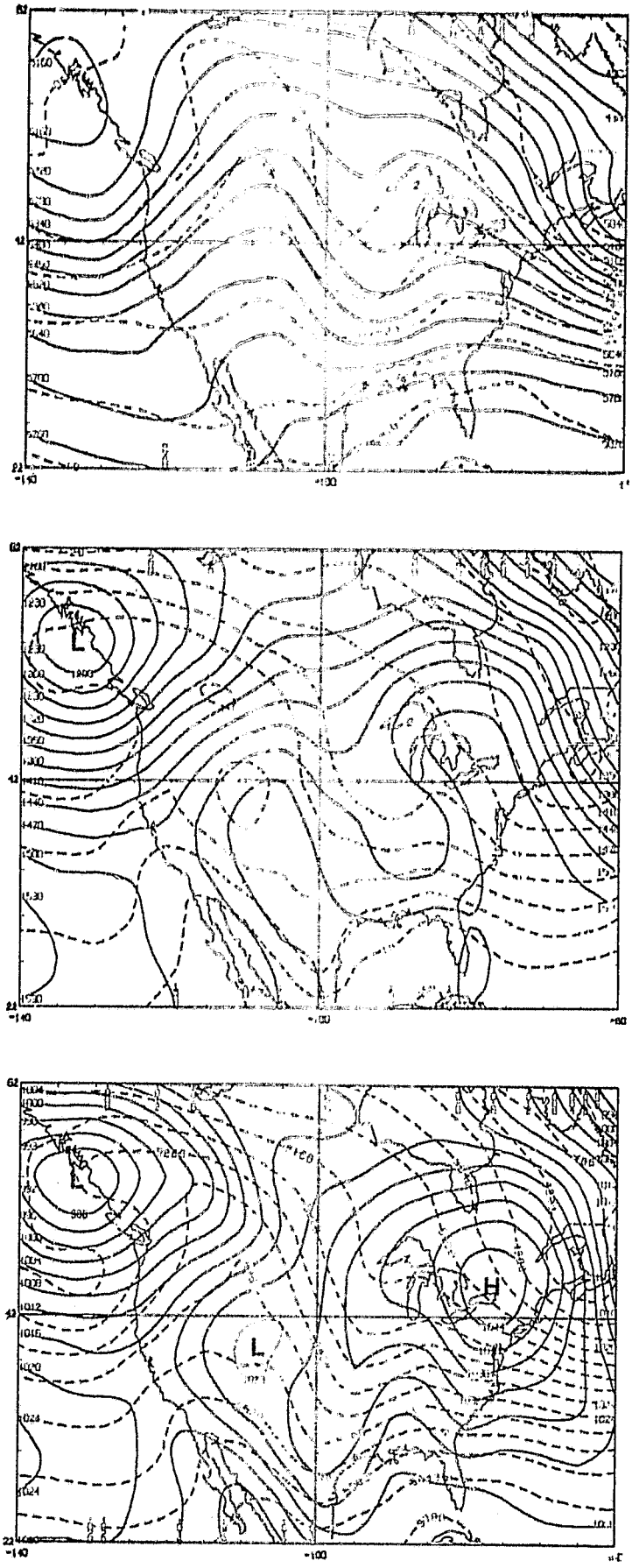

Fig. 19 Same as Fig. 9 for 12 h GLAS model forecast without surface moisture flux from the GLAS analysis at 0000 GMT 18 February 1979.

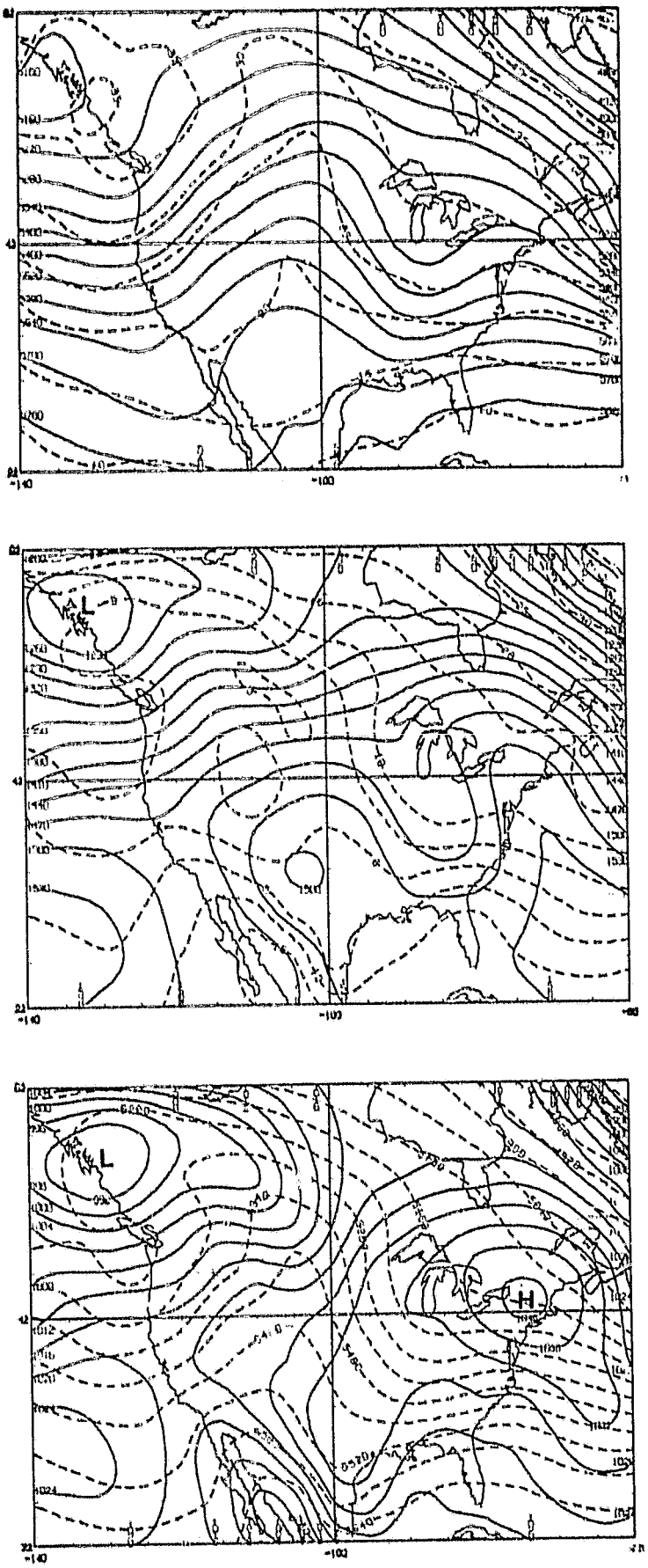

Fig. 20 Same as Fig. 9 for 24 h GLAS model forecast without surface moisture flux from the GLAS analysis at 0000 GMT 18 February 1979.

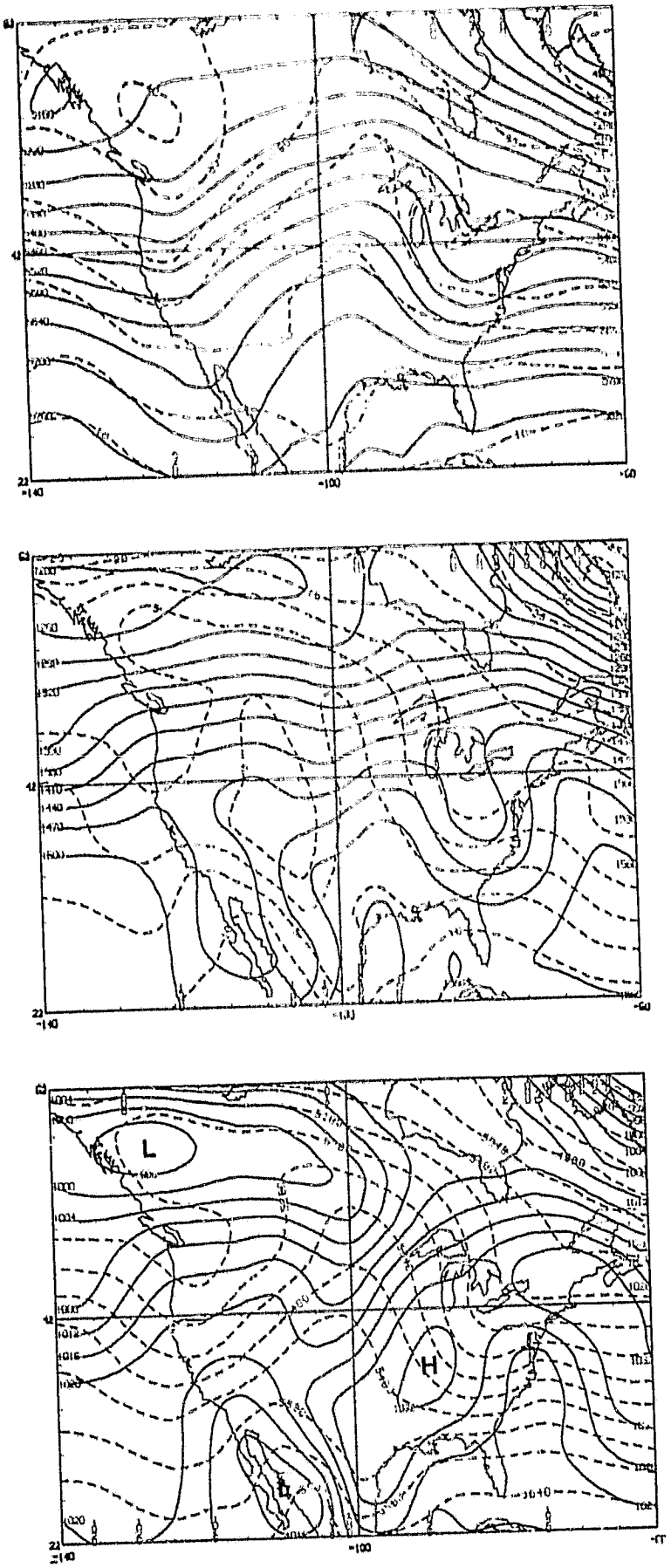

Fig. 21 Same as Fig. 9 for 36 h GLAS model forecast without surface moisture flux from the GLAS analysis at 0000 GMT 18 February 1979.

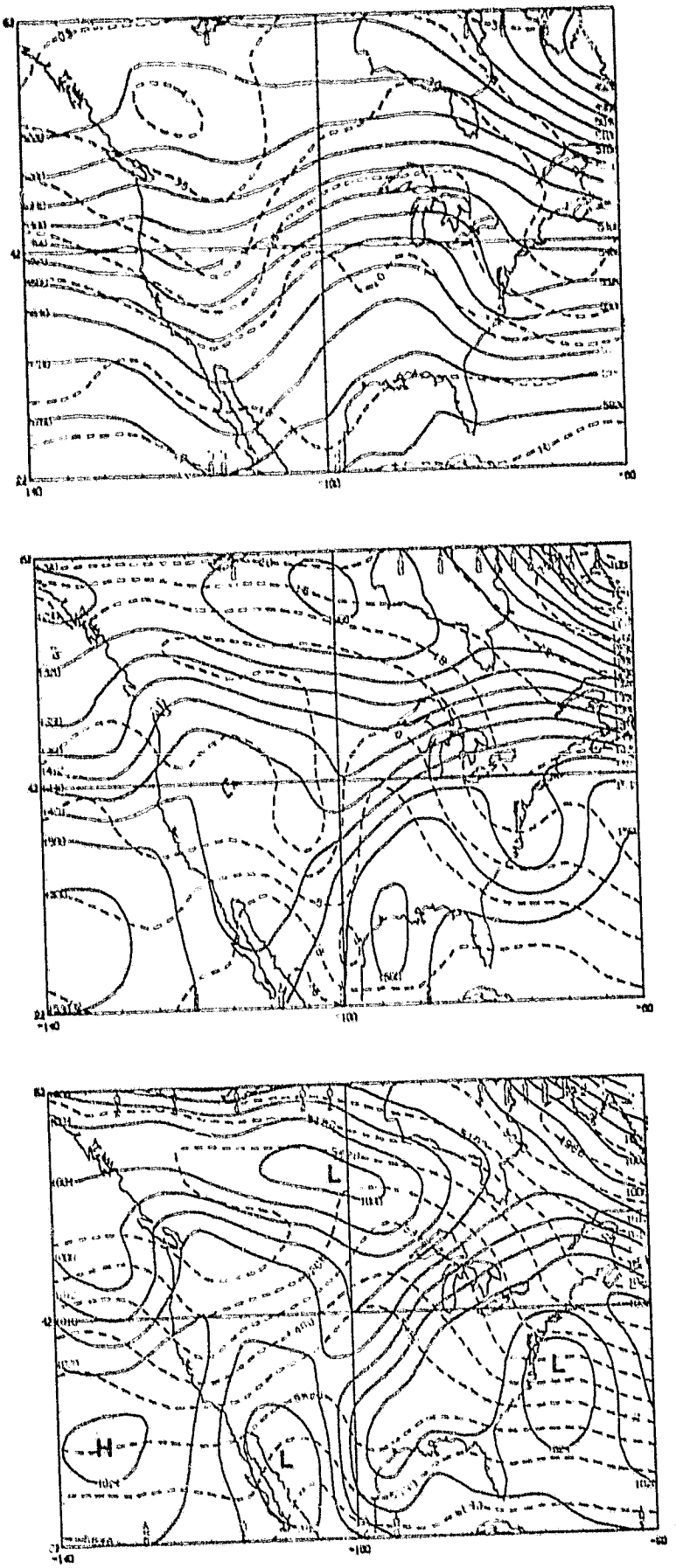

Fig. 22 Same as Fig. 9 for 48 h GLAS model forecast without surface moisture flux from the GLAS analysis at 0000 GMT 18 February 1979.

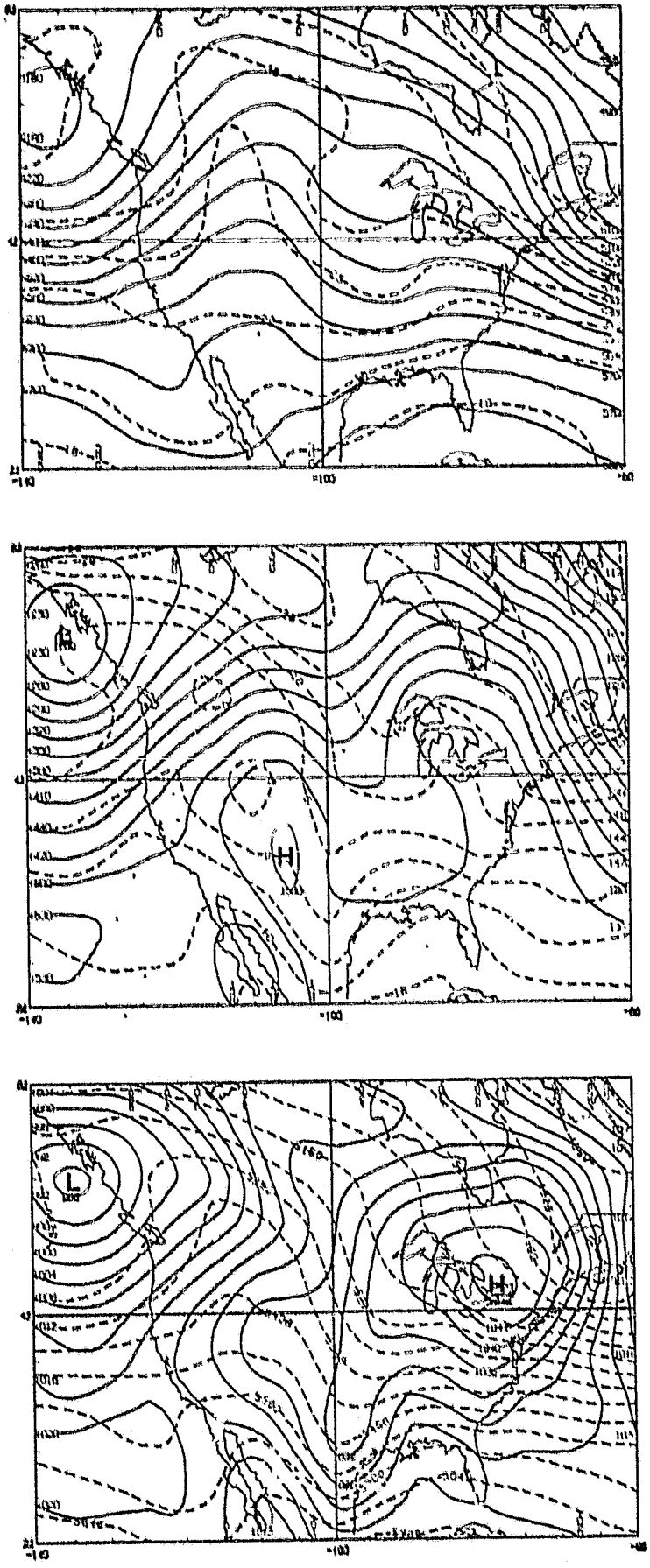

Fig. 23 Same as Fig. 9 for 12 h GLAS model forecast from the NMC analysis at 0000 GMT 18 February 1979.

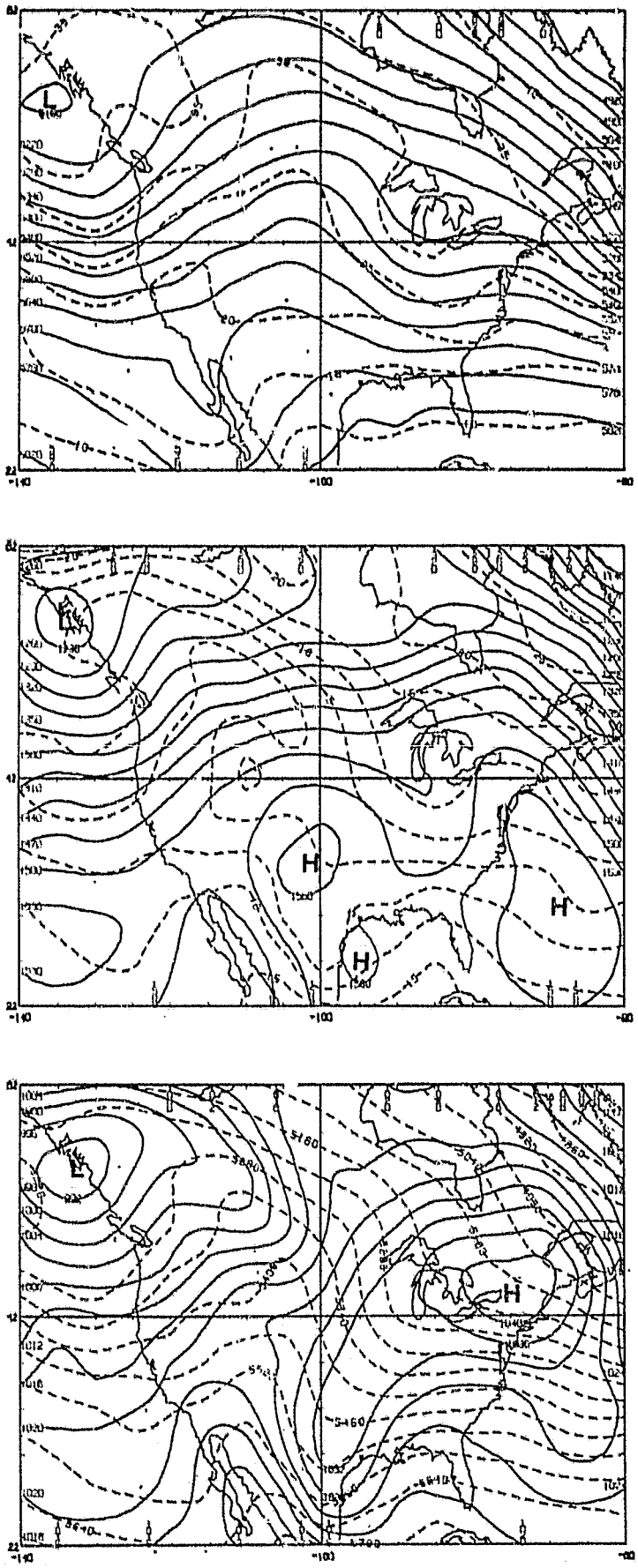

Fig. 24 Same as Fig. 9 for 24 h GLAS model forecast from the NMC analysis at 0000 GMT 18 February 1979.

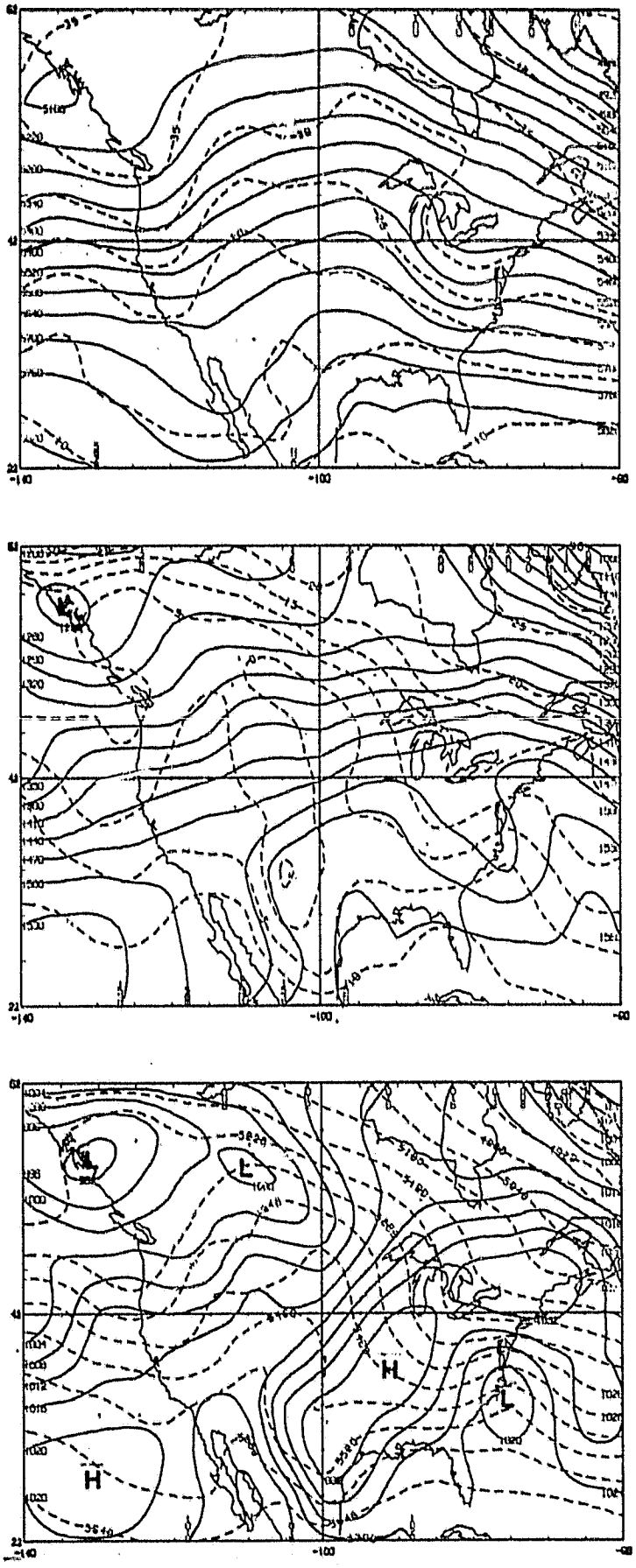

Fig. 25 Same as Fig. 9 for 36 h GLAS model forecast from the NMC analysis at 0000 GMT 18 February 1979.

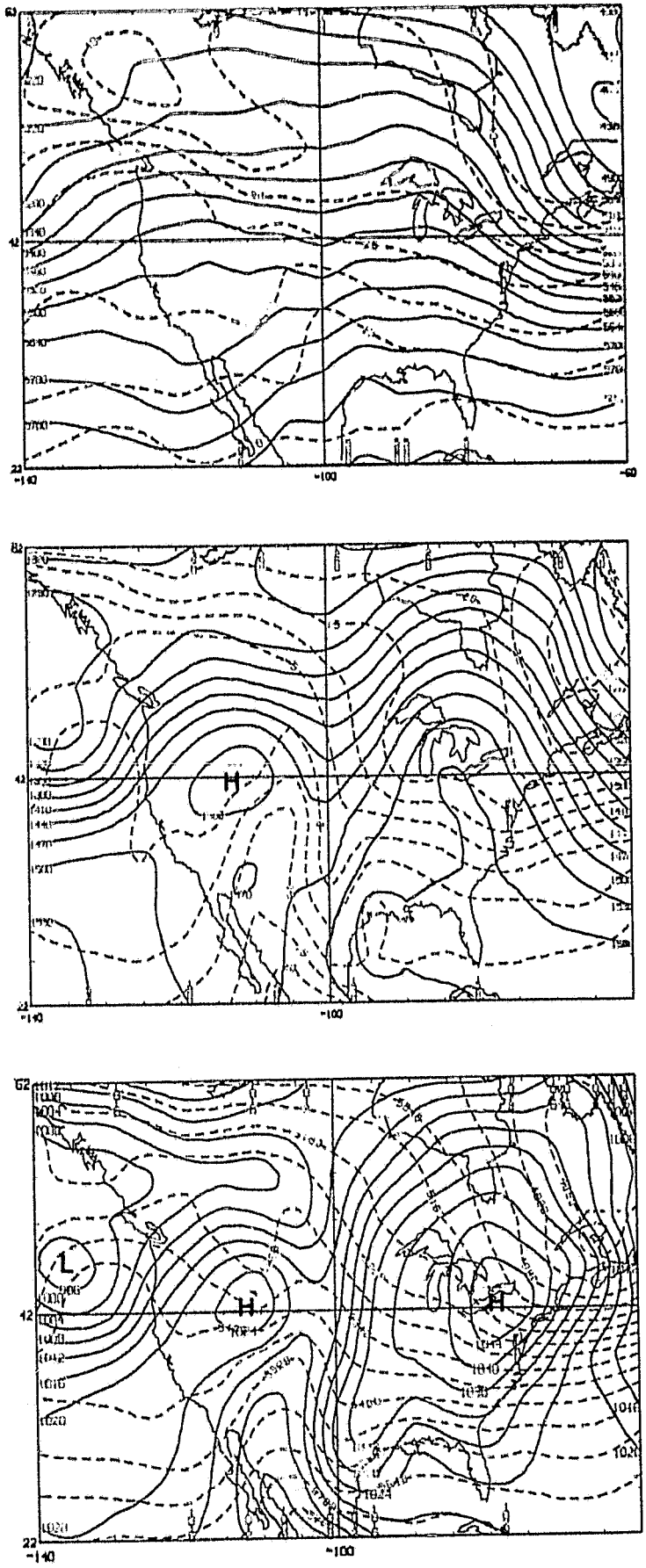

Fig. 26 Same as Fig. 9 for 48 h GLAS model forecast from the GLAS analysis at 0000 16 February 1979.

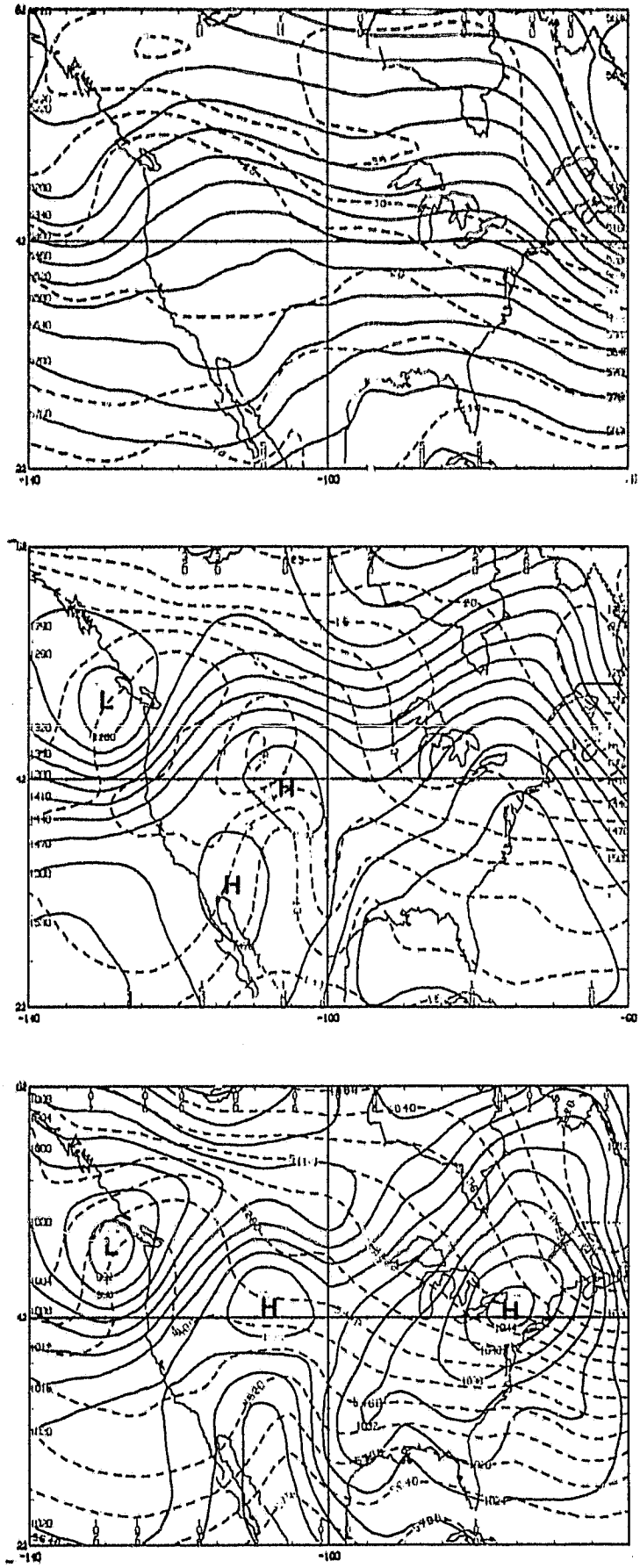

Fig. 27 Same as Fig. 9 for 60 h GLAS model forecast from the GLAS analysis at 0000 GMT 16 February 1979.

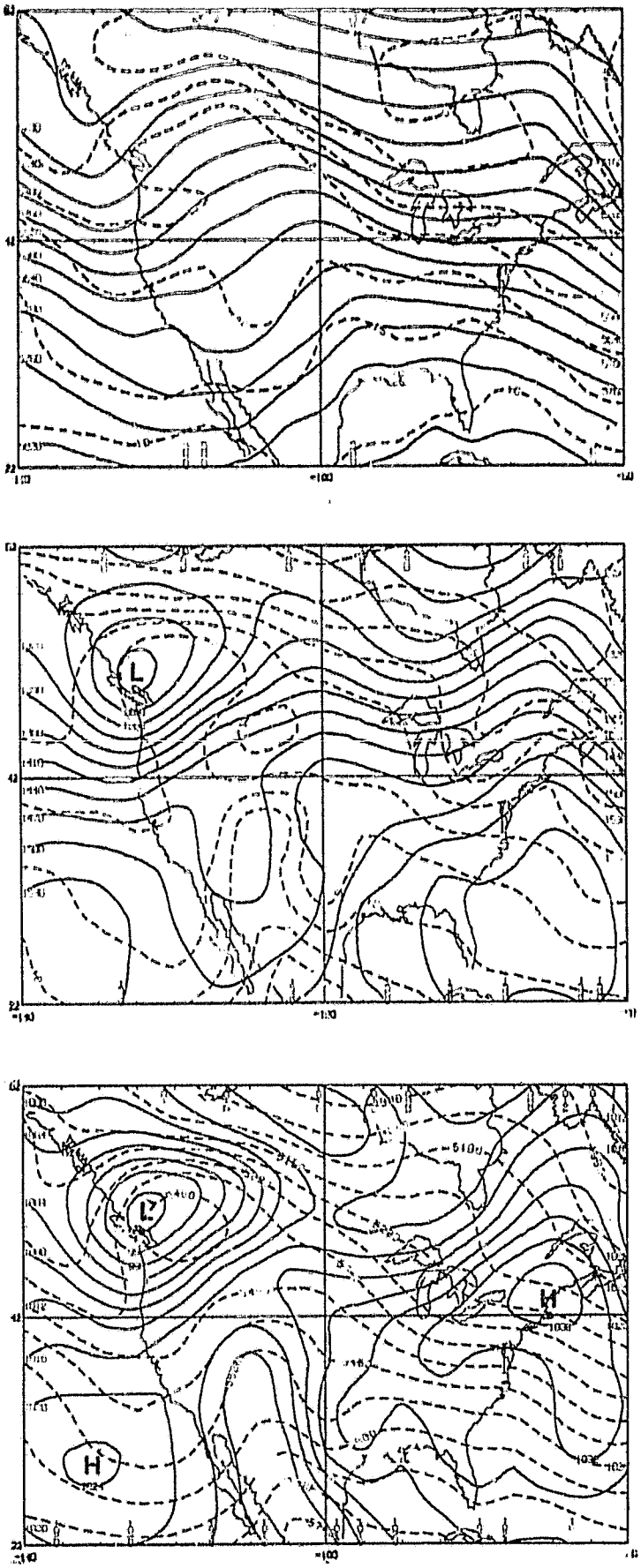

Fig. 28 Same as Fig. 9 for 72 h GLAS model forecast from the GLAS analysis at 0000 GMT 16 February 1979.

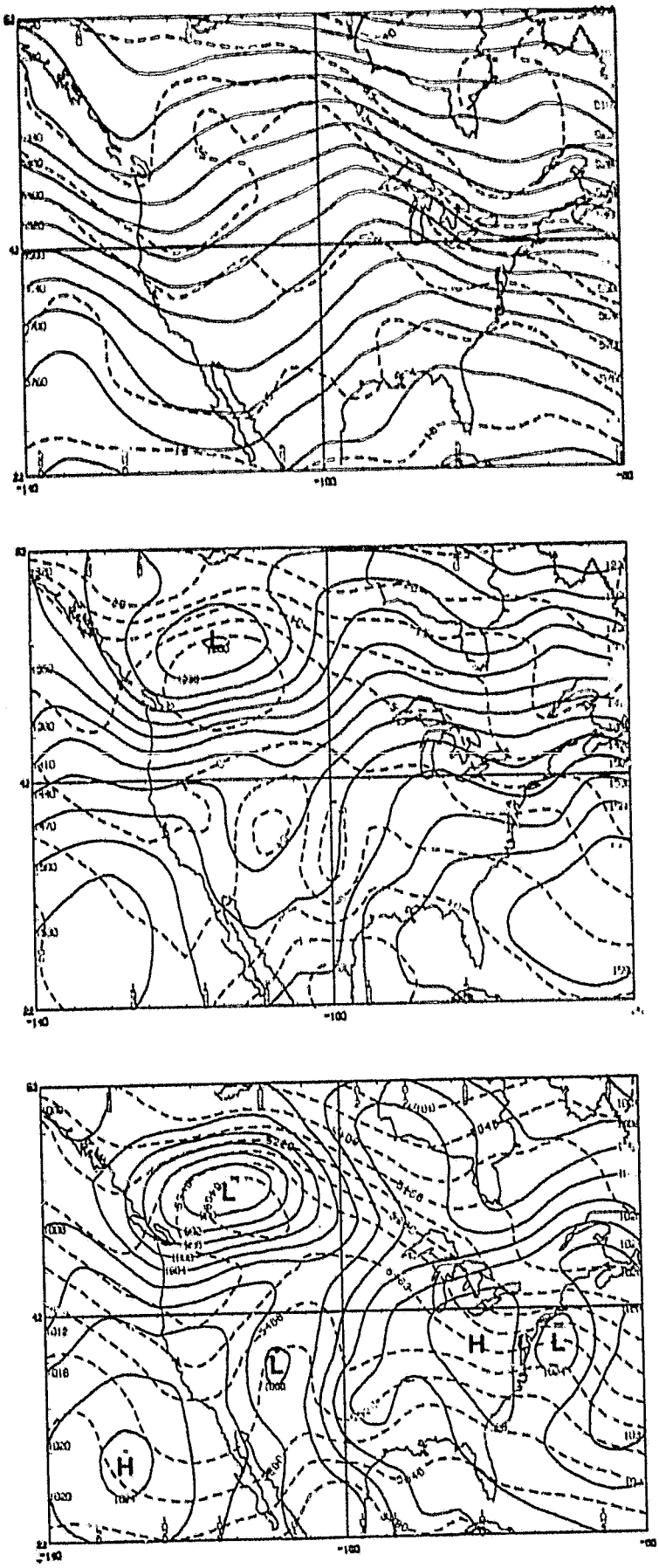

Fig. 29 Same as Fig. 9 for 84 h GLAS model forecast from the GLAS analysis at 0000 GMT 18 February 1979.

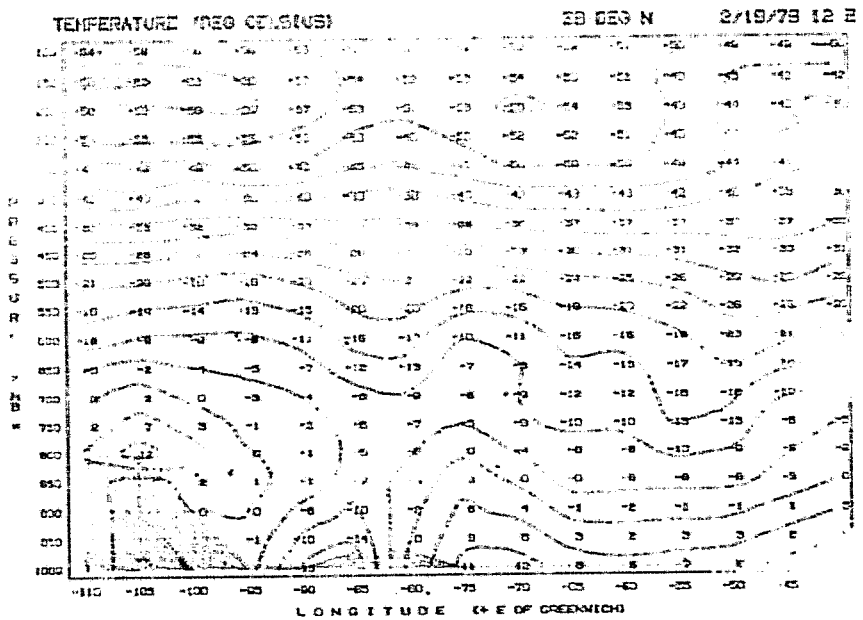

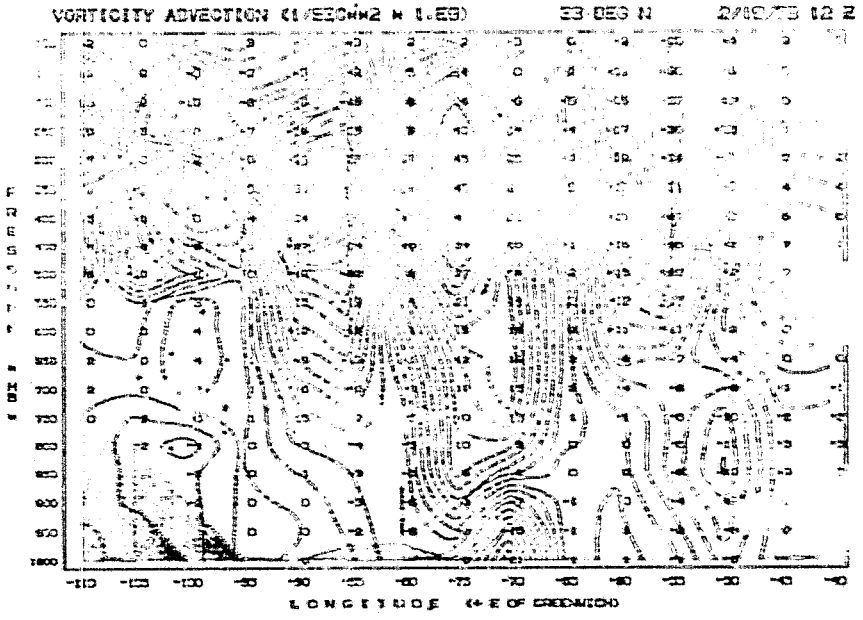

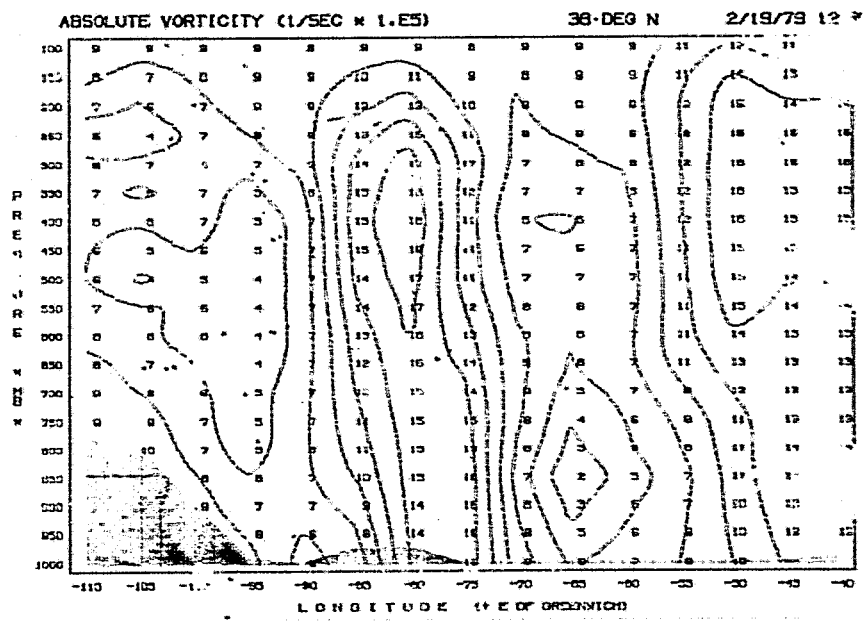

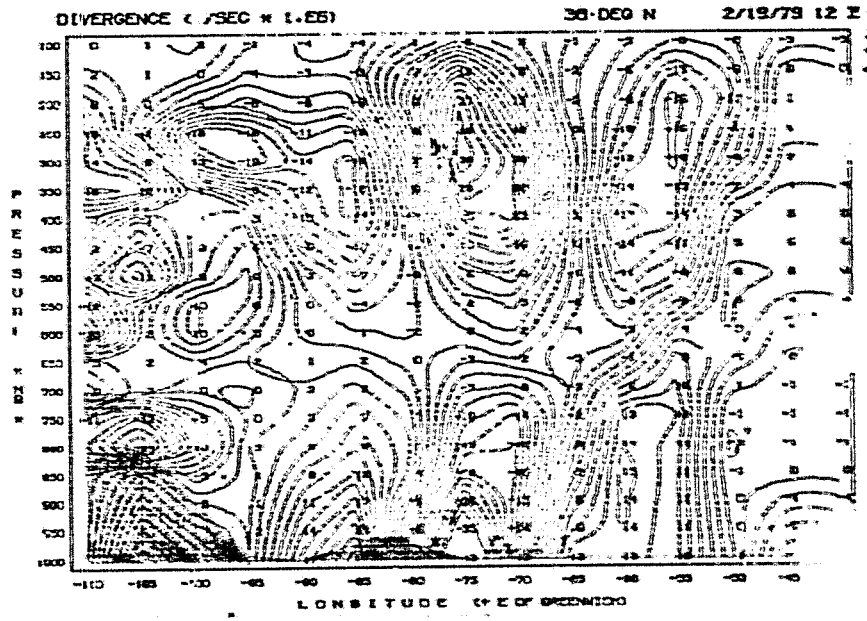

Fig. 30 Vertical cross sections of temperature, absolute vorticity, vorticity advection, and divergence along latitude 38° N for the 36 h GLAS model forecast from the GLAS analysis at 0000 GMT 18 February 1979.

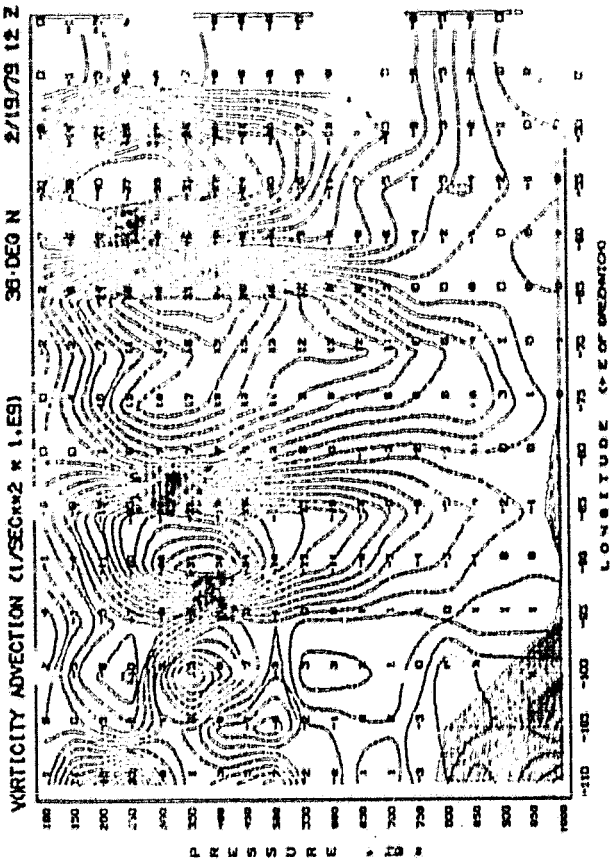

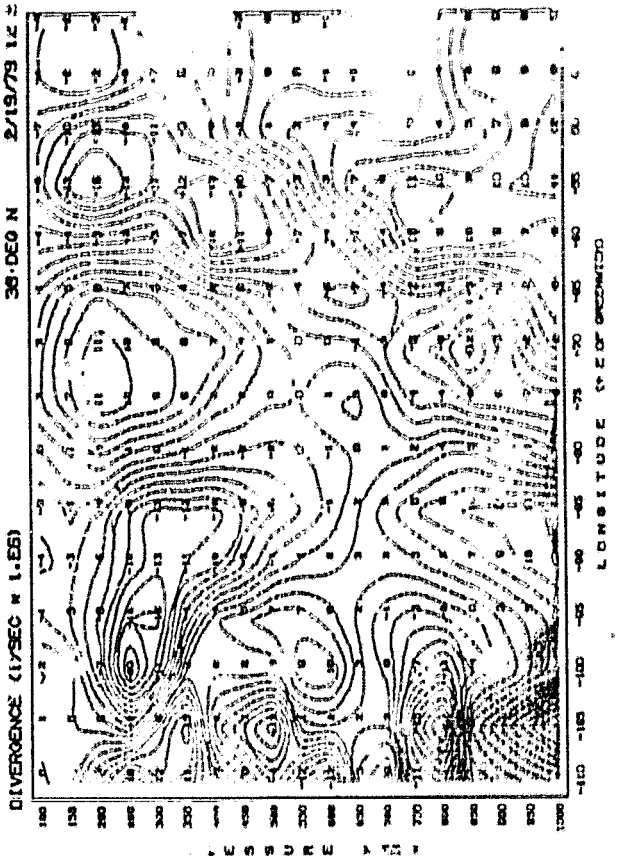

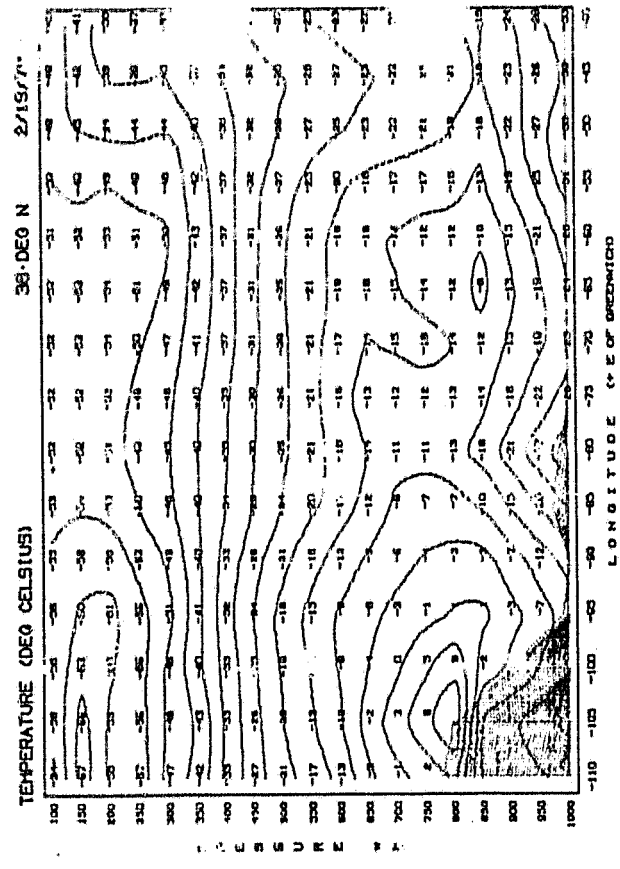

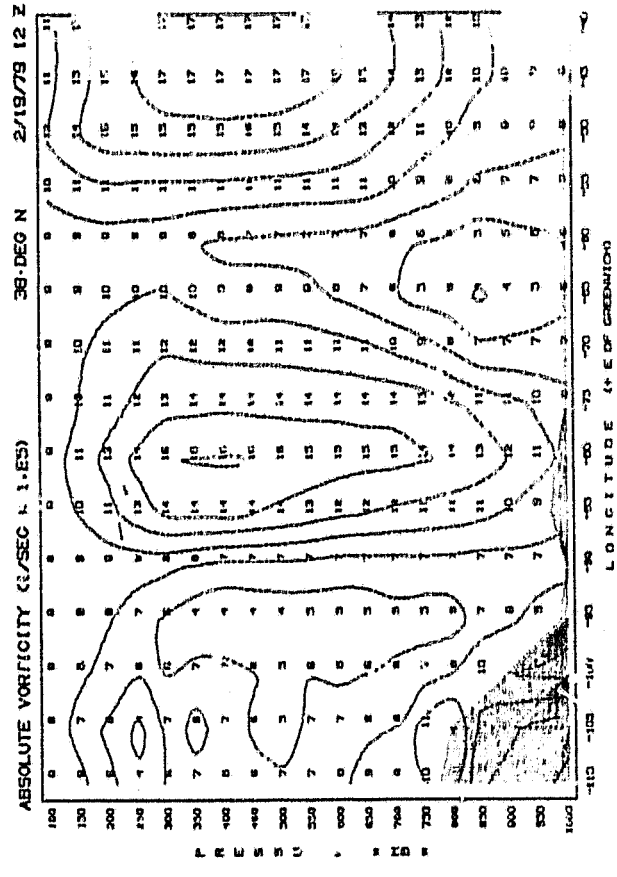

Fig. 31 Same as Fig. 30 for 36 h forecast without surface sensible heat and moisture fluxes.

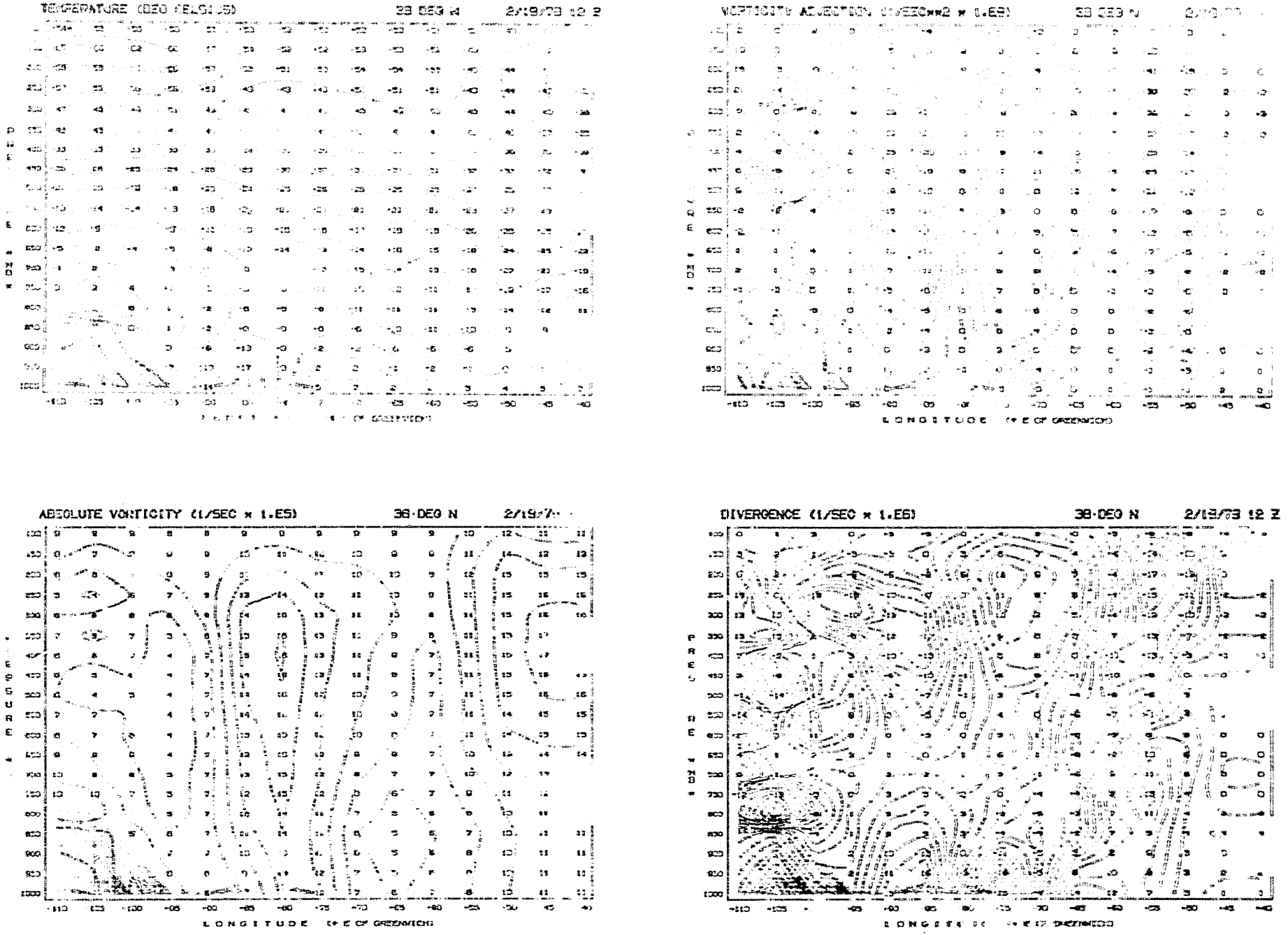

Fig. 32 Same as Fig. 30 for 36 h forecast without surface evaporation.

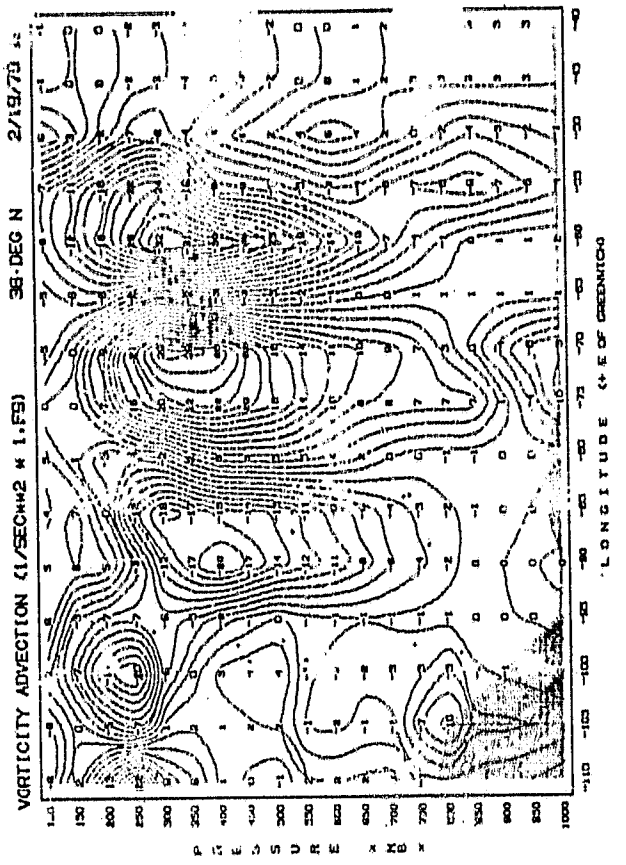

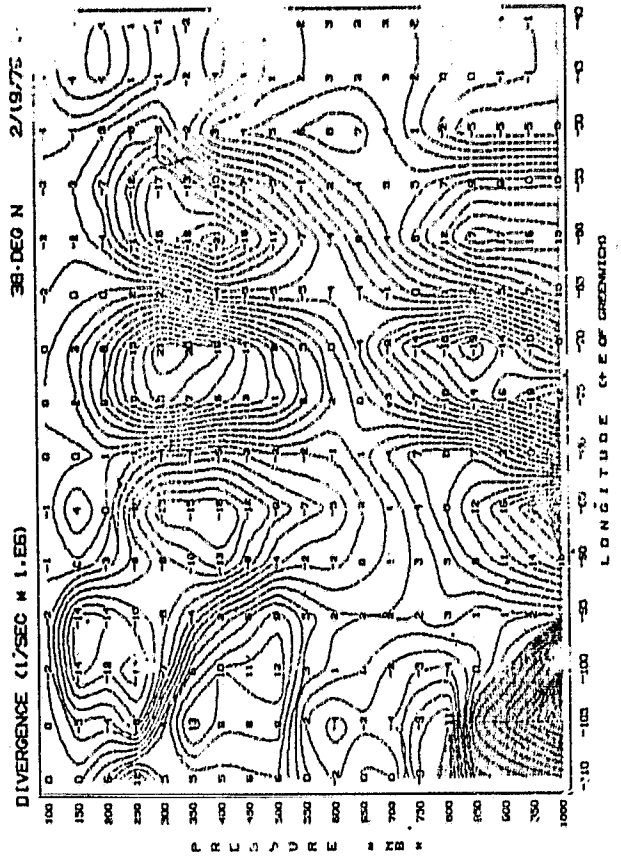

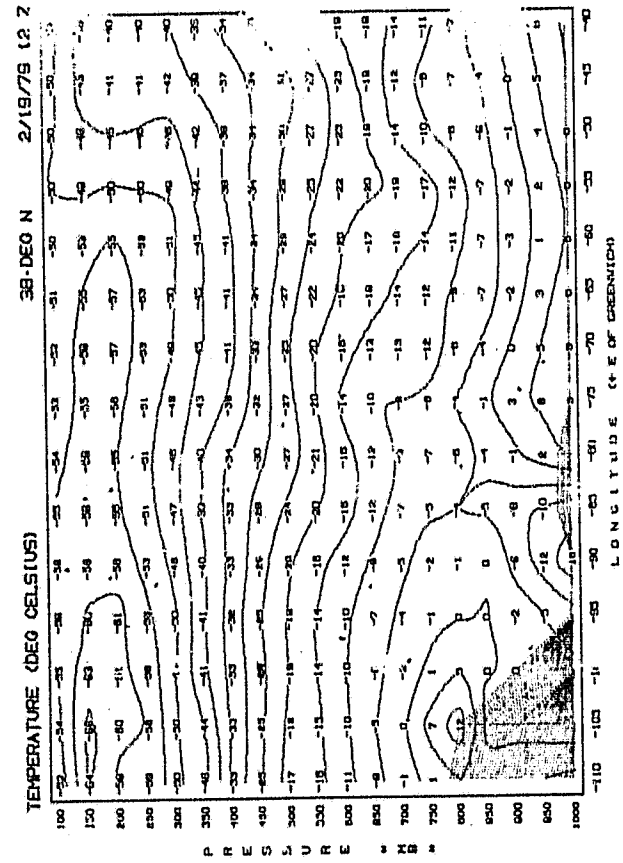

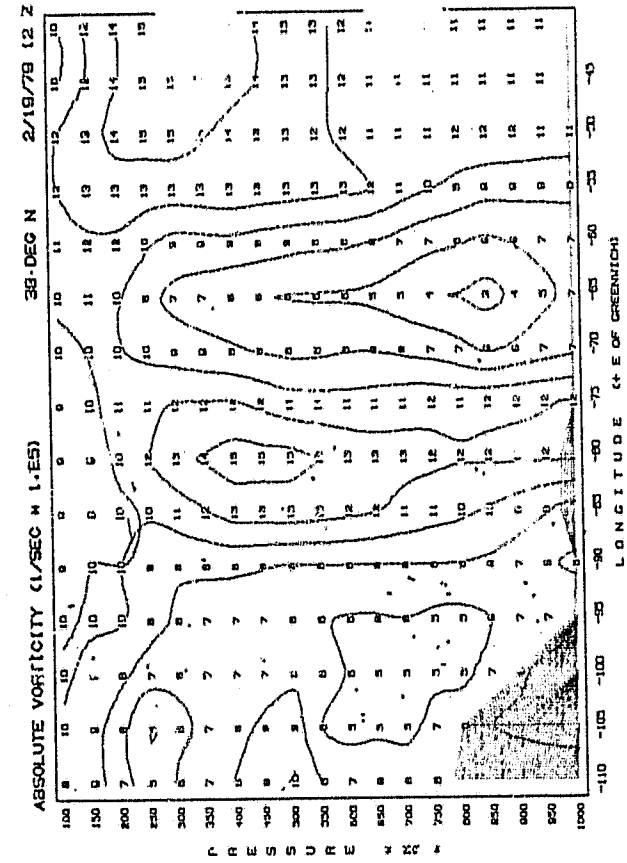

Fig. 33 Same as Fig. 30 for 36 h forecast from the NMC analysis.